Accuracy of the electron pump

H. Dalsgaard Jensen* and John M. Martinis
Electromagnetic Technology Division, National Institute of Standards and Technology, Boulder, Colorado 80303
(Received 15 April 1992)

We calculate the accuracy of the single electron pump numerically and analytically. With a biasing of the device that we describe as optimal, the accuracy is computed with finite temperature cotunneling rates that systematically include all possible cotunneling processes. A simple graphical representation of the operation of the pump illustrates when cotunneling processes become active. We show that the accuracy is limited by cotunneling, thermal activation, and operating the device at too high a frequency; simple approximation formulas are given for these errors. Metrological accuracy is attainable for devices with five or more junctions and with parameters that are experimentally attainable.

I. INTRODUCTION

The Coulomb blockade of tunneling in extremely small junctions has made electronic circuits based on single electrons[1–3] possible. In recent years several practical circuits have been demonstrated, including an electrometer with subelectron sensitivity[4] and three devices that produce a standard of current by locking the transfer of single electrons to a periodic signal.[5–7]

Practical metrological applications of a current standard require an accuracy from about one part per million to one part per billion. The utilization of a current standard is presently thought to be very difficult because small currents are produced in these devices. However, if the devices are used as a charge standard to transfer a controlled number of electrons into a capacitor, then a practical metrological experiment may be possible.[8] If the capacitor is charged with a known number of electrons and its voltage is measured by the Josephson effect voltage standard, the capacitance is then defined through the constant e^2/h. This capacitor can then be used as a primary reference or compared with the calculable capacitor to measure the fine structure constant.[8]

Accuracy predictions are needed to properly design devices as well as to test their performance when built. Simple analytical expressions for the accuracy are desirable, even if they are only approximate, because device parameters then can be easily chosen and any compromises of performance can be readily understood.

At this time, we think the turnstile[6] and pump[7] devices show the greatest promise for an accurate current or charge standard. Of these two devices, we think the pump will make a better standard. Because signals are applied to the gates between every junction in the pump, we think each junction will be more optimally biased than the turnstile device where only the center gate is biased. Additionally, the pump is expected to have less self-heating because the junctions switch closer to their threshold voltages. Therefore, we concentrate in this paper on predicting the accuracy of the pump device. The numerical methods can be simply extended to the turnstile if desired.

It has been suggested that single electrons might be exploited in extremely dense logic circuits which use electrons as the bits of information.[3] Such circuits would probably require error rates much smaller than the rates needed for metrological accuracy. Although the numerical methods we describe in this paper would have to be extended to calculate the error rates in digital circuits, we think that these calculations for the pump device clearly show that several junctions are needed per logic element to reduce the error rates.

A physical process that can significantly affect the accuracy of single electron devices is cotunneling, also called the macroscopic quantum tunneling of charge.[9] In this process an electron is transferred through a Coulomb barrier by virtual states. The first turnstile and pump devices are thought to be limited in accuracy by this effect. The main difficulty in calculating the accuracy comes from cotunneling, and much of this paper is devoted to systematically including in the calculation all possible cotunneling processes.

Pothier[10] has calculated the errors in a pump device at zero voltage and zero temperature. These results give a fairly good prediction of the necessary junction parameters, the basic scaling properties of the cotunneling error rates, and errors due to failure to tunnel. However, for any realistic experiment the device must operate with high accuracy in a small voltage range, and thus a prediction is needed for finite voltages. This is especially important because the accuracy of the electron pump is strongly dependent on the bias voltage. Similarly, a calculation valid for finite temperatures is also needed since it is not presently possible to make the tunnel junctions small enough that the temperature errors can simply be ignored.

Other concerns with the analysis of Pothier are whether it included all possible cotunnneling processes and whether there are any additional error processes which were not taken into account. Thus, for the purposes of this paper, we require a very systematic derivation for the accuracy of the pump. This is accomplished

in part with a computer program which predicts the current-voltage characteristics of the pump by automatically including all possible tunneling and cotunneling processes. In our analytic approach, we calculate thresholds and rates for all possible processes, and then systematically take into account only those that dominate the errors. A comparison of the analytic results with the computer program then checks the derivation.

The structure of the paper is as follows. In Sec. II we begin with a short review of the Coulomb blockade. We also review cotunneling and present an approximation that accounts for the electron-hole excitation energies. This approximation gives a better formula for the cotunneling currents. In Sec. III we describe a computer program for calculating the current-voltage characteristics of the pump. The program takes into account all possible cotunneling processes and is valid for finite temperatures. We then derive in Secs. IV and V analytical expressions for the accuracy by considering an ideal array of small junctions. We derive the optimum biasing of the device. We then systematically characterize the cotunneling processes and identify the regions in which the various processes occur as a function of the bias parameters. Finally, in Sec. VI we analyze the error processes in the region of smallest errors and derive both full and simple analytical formulas for the accuracy. The simple formulas are then used to choose device parameters for target accuracies of one part per million and one part per billion. In the appendixes we elaborate on several details of the derivation.

II. COULOMB BLOCKADE IN MULTIJUNCTION CIRCUITS

A. Single junction

We will first review the basic predictions of the Coulomb blockade for an idealized model of a small capacitance tunnel junction connected to a charge bias Q, as shown in Fig. 1(a). In the absence of tunneling, the tunnel junction behaves simply as a capacitance C. In Figs. 1(b) and 1(c) we show that the effect of a tunneling event is to transfer a charge of $\pm e$ across the junction, where e is the charge of an electron and the $\pm$ indicates the direction of tunneling. Since the tunneling of an electron is equivalent to changing the total charge bias to $Q \pm e$, the energies of the two final states are simply the energy of the initial state $Q^2/2C$ with Q replaced by $Q \pm e$. Figure 1(d) plots the energy of the initial state and the two final states as a function of the bias charge Q. For a $+e$ transition in this single junction the Coulomb energy change

$$\Delta E_1 = U_{(\text{final})} - U_{(\text{initial})} = \frac{e}{C}\left(\frac{e}{2} - Q\right) \quad (1)$$

is positive for $Q < e/2$, whereas for the $-e$ transition ΔE_1 is positive for $Q > -e/2$.

An electron tunneling across the junction starts from a filled state on one side of the junction and then occupies an empty state on the other side. The energy of this electron-hole excitation and the Coulomb energy change ΔE_1 must add to zero. The current in this direction is given by first-order perturbation theory to be the tunneling matrix element summed over all the possible transitions

$$I_+ = 2e\frac{2\pi}{\hbar}\int_{-\infty}^{+\infty}\int_{-\infty}^{+\infty} |M|^2 \rho_1(\varepsilon_1)\rho_2(\varepsilon_2) f(\varepsilon_1) f(\varepsilon_2) \times \delta(\varepsilon_1 + \varepsilon_2 + \Delta E_1) d\varepsilon_1 d\varepsilon_2 = \frac{-\Delta E_1}{eR_T}\frac{1}{1-\exp(\Delta E_1/k_B T)}, \quad (2)$$

where the factor of 2 is due to spin, $\rho_{1,2}$ is the electron density of states of the two sides of the junction and is assumed constant for the metal electrodes making up the junction, f is the Fermi function, and M is the tunneling matrix element. In Eq. (2) we have defined a phenomenological constant $R_T = R_K/(8\pi^2|M|^2\rho_1\rho_2)$ as the junction resistance. The resistance quantum is $R_K = h/e^2 \approx 25.8$ kΩ. This junction resistance is the experimentally measurable parameter that describes the total coupling strength of the tunnel junction. In our notation, where ΔE_1 is the change in Coulomb energy, $-\Delta E_1$ has *positive* magnitude for allowed transitions at $T = 0$; hence the minus sign in Eq. (2).

Equations (1) and (2) predict that for $k_B T \ll e^2/2C$, no current can flow through the junction when ΔE_1 is positive, which corresponds to $|Q| < e/2$. This is the Coulomb blockade of tunneling current.

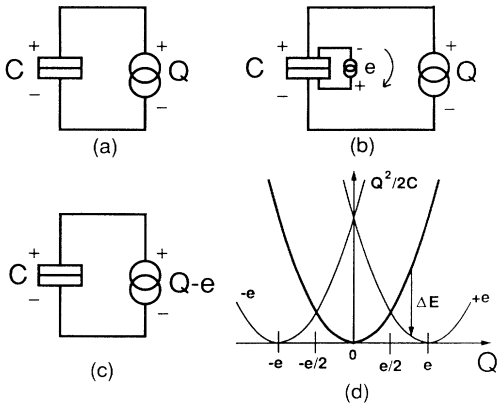

FIG. 1. The basic model of a small capacitance tunnel junction with a charge bias. The box symbol represents the tunnel junction. Figure (a) is the basic model, (b) the junction after tunneling of a charge e in the forward direction, (c) the equivalent circuit after tunneling, and (d) the Coulomb energy of the initial state and the two possible final states as function of the charge bias. The energy difference ΔE associated with a tunneling event is shown by the arrow.

B. Multijunction circuit

We now consider the Coulomb blockade for the general series array of junctions shown in Fig. 2(a). In this circuit, an array of tunnel junctions is connected to an

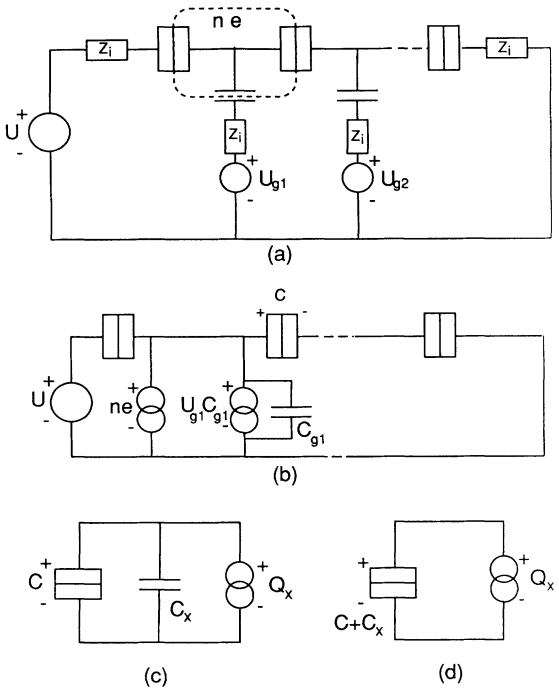

FIG. 2. A general circuit for a series array of small tunnel junctions connected to voltage sources by impedances Z_i. Figure (a) is the circuit model, (b) the circuit after removing the low impedance leads and representing the electrons on the islands as charge sources, (c) the circuit as it would appear to the junction labeled C, reduced from the Norton equivalence theorem to be an external charge Q_x and an external capacitance C_x, and (d) the final reduction which can be compared to Fig. 1(c).

array of voltage sources. The source impedances $Z_i(\omega)$ model the effect of the electromagnetic environment of the leads. The electrodes connecting junctions and capacitances are "islands" on which excess electrons may be trapped.

The effect of the environment on the Coulomb blockade has been calculated for single[11] and multijunction[12] circuits. For a single junction circuit with a real environmental impedance $Z \ll R_K$, the tunneling rate with the environmental impedance[12] compared to the rate with $Z = 0$ is for voltage $V \lesssim e/C\alpha$

$$\frac{\Gamma|_\alpha}{\Gamma|_{\alpha=0}} \simeq \frac{1}{(1+\alpha)\Gamma(1+\alpha)} \left(\frac{\pi e^{-\gamma}\alpha V}{e/C}\right)^\alpha, \tag{3}$$

where $\alpha = 2Z/R_K$ and $\gamma = 0.577...$ is the Euler constant. The leads in a real experimental circuit have a complex and frequency-dependent impedance at the appropriate microwave frequencies but can be approximated reasonably well by a real impedance of $Z_i \sim 100\ \Omega$. The tunneling rate is thus approximately 5% less than the zero impedance rate. A calculation for a multijunction circuit gives a similarly small effect. Thus, we can safely set all the impedances $Z_i(\omega) = 0$.

The excess electrons on the islands can be modeled by charge sources from ground to the island with magnitude of an integral number of unit charges. This allows us to treat in the same manner the charge trapped on islands and charge induced there by the gate voltage sources. Thus, Fig. 2(a) reduces to Fig. 2(b).

We now consider the Coulomb energy change of the system in Fig. 2(b) for an electron tunneling across the junction labeled with a capacitance C. Since we are considering charge transfer only through this junction, all other junctions behave as capacitors. In this case, we can further simplify the circuit through the use of the Norton equivalence theorem, which states that an arbitrary two-port circuit of capacitors, charge sources, and voltage sources can be represented by a capacitor C_x and a charge bias source Q_x.[13] Thus, junction C in Fig. 2(b) can be represented as Fig. 2(c), which can be further simplified to Fig. 2(d). The Coulomb energy change for Fig. 2(d) is exactly that depicted in Fig. 1(a), where the Coulomb energy due to a $\pm$ electron transition changes by

$$\Delta E_1^{\pm} = \frac{e}{C + C_x}\left(\frac{e}{2} \mp Q_x\right). \tag{4}$$

The difficulty in computing ΔE_1 is reduced with this technique to finding the Norton equivalent circuit parameters C_x and Q_x. As we shall see, the symmetry of the pump circuit allows us to calculate these quantities easily. The relation between the external charge and the charge on the junction itself is simply

$$Q_{\text{junction}} = \frac{C}{C + C_x} Q_x. \tag{5}$$

C. Dynamic equations

The electrical characteristics of a tunnel junction circuit can be computed using a master equation technique.[2] In this technique, all the possible states of the circuit are given by a set of coordinates $\mathbf{n} = (n_1, n_2, ...)$ that defines the number of excess electrons on each island. For a series array of N junctions, the system state is given by the $(N-1)$-dimensional vector $\mathbf{n} = (n_1, n_2, ..., n_{N-1})$. Each n_i can in principle be an integer number from $-\infty$ to ∞. The system dynamics can then be described in terms of a vector $\mathbf{P}$; the elements P_n give the probability that the system is in state n, where n is an index for the state vector $\mathbf{n}$. The change of a state with time is calculated by knowing the rates Γ_{nm} for an initial state $\mathbf{n} = (n_1, n_2, ...)$ to go to a final state $\mathbf{m} = (m_1, m_2, ...)$. Thus, the master equation is

$$\frac{dP_n}{dt} = \sum_m \Gamma_{mn} P_m - \sum_m \Gamma_{nm} P_n, \tag{6}$$

which may be cast into a simple matrix equation

$$\frac{d}{dt}\mathbf{P} = \mathbf{\Gamma} \cdot \mathbf{P}, \tag{7}$$

where $(\mathbf{\Gamma})_{ij} = \Gamma_{ji}$ and $(\mathbf{\Gamma})_{ii} = -\sum_{j\neq i}\Gamma_{ij}$ is the transition rate matrix. Because there may be several ways in which the system can go from a state n to a state m, each of the Γ_{nm} is a sum of the rates for these individual processes.

Lowest-order perturbation theory, valid to order $1/R_T$, gives the result in Eq. (2), which predicts that an electron can tunnel across only one junction at a time. Averin and Odintsov[9] have extended perturbation theory to calculate rates to higher order in $1/R_T$. This higher-order perturbation theory shows that electrons can tunnel across several junctions at the same time in a process called cotunneling. Single junction tunneling is a special case in this general treatment. We consider here only inelastic cotunneling where different electron states participate in each of the single-junction tunneling processes that makes up the cotunneling event. Elastic cotunneling rates[14] are expected to be negligibly small for typical metallic junctions that would be used initially.

D. Cotunneling

We may understand cotunneling by considering an arbitrary long sequence of single-junction tunneling events $(j_1, j_2, ..., j_n)$, where j_i is a number $\pm 1, ..., \pm N$ that represents a junction and the direction of tunneling. Because of the linearity of the capacitive circuit, the change in Coulomb energy ΔE_k from the initial state to the state after the kth event is given by $\Delta E_k = \sum_{i=1}^{k}\delta E_i$. The change in energy δE_i associated with each of the tunnel events in the sequence is calculated from Eq. (4) given the equivalent circuit parameters Q_x and C_x. After each tunneling event the system is in a new state, with a new distribution of electrons on the islands, and a new determination of Q_x is required to calculate the change in energy for the *next* tunneling event.

We may diagrammatically represent cotunneling, the intermediate states, changes in energy due to tunneling, and the total change in Coulomb energy as shown in Eq. (8).

$$\begin{array}{lll} & \text{event :} & \quad j_1 \qquad\quad j_2 \qquad\quad j_3 \\ \text{sequence } (j_1,j_2,j_3): & \text{state :} & m \longrightarrow s_1 \longrightarrow s_2 \longrightarrow n \\ & & \quad \delta E_1 \qquad \delta E_2 \qquad \delta E_3 \\ & \text{energy :} & 0 \qquad \Delta E_1 \qquad \Delta E_2 \qquad \Delta E_3 \end{array} \tag{8}$$

For the initial state m we set the energy equal to zero. The first tunneling event j_1 in the process takes the system to the intermediate state s_1, with an associated change in energy of δE_1. The following events j_2 and j_3 take the system through intermediate state s_2 to the final state n, with changes in energy of δE_2 and δE_3. The Coulomb energy of the intermediate states are given by the initial energy plus the change in energy associated with the tunneling event; hence, the final energy is $\Delta E_3 = \delta E_1 + \delta E_2 + \delta E_3$ for the sequence (j_1, j_2, j_3). The final energies ΔE_3 of the permutations of the sequence (j_1, j_2, j_3) are all the same.

At zero temperature Eq. (2) shows that, if $\Delta E_1 > 0$, the tunneling event j_1 cannot occur. However, cotunneling considers transition rates for the state s_1 being a *virtual* state. In this way, cotunneling causes electrons to tunnel simultaneously across many junctions through these virtual states. Transitions from any state n to any other state m are thus allowed as long as the final state is lower in Coulomb energy than the initial state (at zero temperature). The quantum mechanical amplitude for cotunneling is obtained by summing contributions from the $n!$ possible sequences involving that set of junctions. We can refer to a cotunneling event by a tunneling configuration $\{j_1, j_2, ..., j_n\}$: the *set* of single-junction tunneling events.

The prediction for the cotunneling rate for a process composed of n single-junction tunneling events is given by[9]

$$\Gamma^{(n)} = \frac{2\pi}{\hbar}\left(\prod_{i=1}^{n}\frac{R_K}{(2\pi)^2 R_{Ti}}\right)\int_0^\infty S^2(\omega_1,...,\omega_n)\delta\left(\Delta E_n - \sum_{i=1}^{2n}\omega_i\right)\left(\prod_{i=1}^{2n} f(\omega_i)d\omega_i\right), \tag{9}$$

where δ is the Dirac delta function and S is a factor of the tunneling matrix element given by

$$S = \sum_{\text{perm}\{j_1,...,j_n\}}\prod_{k=1}^{n-1}\frac{1}{\varepsilon_k}. \tag{10}$$

Each permutation of the tunneling configuration $\text{perm}\{j_1, ..., j_n\}$ gives rise to a tunneling sequence (path) with the intermediate energies ε_k given by

$$\varepsilon_k = \Delta E_k + \sum_{i=1}^{2k}\omega_i, \tag{11}$$

where ΔE_k is the change in Coulomb energy after the kth event in the sequence and $\omega_{2k-1} + \omega_{2k}$ is the electron-hole excitation energy of that event. The expansion parameter of the cotunneling theory is R_K/R_T, thus requiring that $R_T \gg R_K$.

Because the integration involves the Fermi functions as well as the energy denominators in Eq. (10), Eq. (9) cannot be explicitly integrated except for the case of $n = 2$ at zero temperature.[9] For the two-junction case, the result gives a logarithmic divergence as ΔE_1 approaches zero, which corresponds to the voltage approaching the threshold of single-junction tunneling. The divergence arises from a breakdown of perturbation theory and is unphysical. At present, theories are being developed to remove this logarithmic divergence and to calculate the cotunneling current above the threshold voltage for single-junction tunneling. In this paper, an approximation described below will remove this divergence.

An approximation, introduced in Ref. 9, valid for final energy $\Delta E_n \to 0$ is obtained by setting the ω terms in the energy denominators to zero. In this approximation,

$$S = \sum_{\text{perm}\{j_1,\ldots,j_n\}} \prod_{k=1}^{n-1} \frac{1}{\Delta E_k}, \tag{12}$$

and the integrals in Eq. (9) involve only the Fermi functions. In this form the integrals can be calculated analytically. A better approximation assumes that the energy difference ΔE_n is, on the average, equally divided over all the electron-hole excitation energies. Thus, $\omega_i = -\Delta E_n/2n$, and Eq. (11) becomes

$$\varepsilon_k = \Delta E_k - \frac{k}{n}\Delta E_n. \tag{13}$$

As when using Eq. (12), the integrals over ω in Eq. (9) can be solved and the result for arbitrary temperature is[15]

$$\begin{aligned} F_n(\Delta E_n, T) &\equiv \int_{-\infty}^{\infty} \delta\left(\Delta E_n - \sum_{i=1}^{2n} \omega_i\right)\left(\prod_{i=1}^{2n} f(\omega_i) d\omega_i\right) \\ &= \frac{\prod_{i=1}^{n-1}\left[(2\pi k_B T \cdot i)^2 + (\Delta E_n)^2\right]}{(2n-1)!} \\ &\quad \times \frac{-\Delta E_n}{1 - \exp\left(\Delta E_n / k_B T\right)}. \end{aligned} \tag{14}$$

For zero temperature the expression reduces to

$$F_n(\Delta E_n, 0) = \frac{(-\Delta E_n)^{2n-1}}{(2n-1)!}\Theta(-\Delta E_n), \tag{15}$$

where $\Theta(x)$ is the step function, and states that a cotunneling process can proceed only if it is energetically favorable. At finite temperature, it is possible for cotunneling to occur with positive energies of order $k_B T$, as is possible for single-junction transitions.

We further justify the approximation used in Eq. (13) by comparing in Fig. 3 the ratio of the cotunneling rate obtained using the approximation Eq. (13) (solid line) and the rate obtained by setting the excitation energies equal to zero (dashed line) to the full result for the cotunneling current for two junctions at zero temperature, Eq. (32) in Ref. 9. We have defined V_t as the voltage for onset of single-junction tunneling. The expression using Eq. (13) closely matches the full result for voltages below $0.9V_t$, where the approximation differs from the full result by less than a factor of 2. When the electron-hole energies are set to zero in the energy denominator, as in Eq. (12), a much less accurate approximation is obtained.

Because the cotunneling theory is based on the assumption that the intermediate states are energetically forbidden, we will consider only cotunneling sequences with intermediate states that cannot be reached by lower-order tunneling. A lower-order process in this context is meant to be a subsequence of the tunneling sequence considered. At zero temperature this implies that sequences are not included when the Coulomb energy of an intermediate state $\Delta E_k < 0$. Similarly, at finite temperatures, we want to exclude sequences with a nonzero rate from the final state to an intermediate state. We approximate

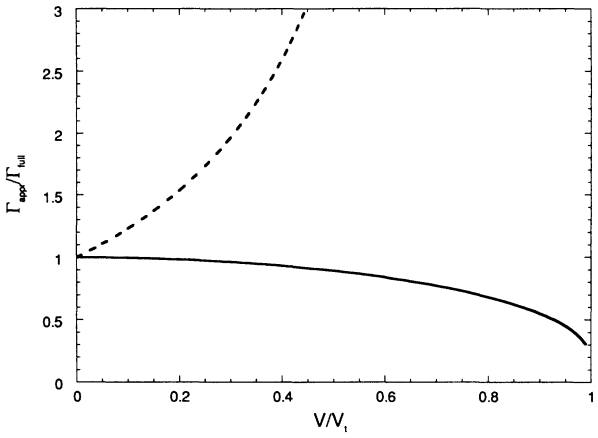

FIG. 3. The voltage dependence of the ratio of two approximations for cotunneling to the full rate given by Eq. (32) in Ref. 9 through two junctions. The threshold voltage for single-junction tunneling is V_t. The approximation obtained by setting the excitation energies equal to zero is the dashed line. The approximation we use distributes the final energy equally among the excitation energies and is the solid line. The ratios are computed at zero temperature.

this condition by requiring all intermediate states to also have higher energies than the final state.

Hence, in this paper we use the following expression for the transition rate for a cotunneling event of order n:

$$\Gamma^{(n)} = \frac{2\pi}{\hbar}\left(\prod_{i=1}^{n} \frac{R_K}{(2\pi)^2 R_{Ti}}\right) S^2 F_n(\Delta E_n, T), \tag{16}$$

where we have defined

$$S = \sum_{\text{perm}\{j_1,\ldots,j_n\}} \left(\prod_{k=1}^{n-1} \frac{1}{\Delta E_k - \frac{k}{n}\Delta E_n} \times \Theta(\Delta E_k - \max(0, \Delta E_n))\right). \tag{17}$$

An *a posteriori* justification for this approximation is that detailed balance is exactly satisfied; that is, $\Gamma_{m\to n} = \exp\left[-\Delta E_n / k_B T\right]\Gamma_{n\to m}$ for all possible transitions. Thus, we think that the energy denominator adopted in Eq. (13) and the energy cutoff defined by the Θ function in Eq. (17) are good approximations.

Because the contribution of a tunneling sequence is cut off abruptly by the Θ function when an intermediate energy crosses the threshold, our prediction for the rate is a poor approximation near threshold. We return to this point later in the paper and show that this approximation does not significantly affect our final results for the accuracy of the pump.

The rate for single-junction tunneling, Eq. (2), is obtained by setting $S = 1$ and $n = 1$ in Eq. (16). Hence we may describe *all* tunnel processes under one formalism, the only difference being the order of perturbation theory. This allows a universal approach in the calcula-

tion of tunneling thresholds, rates, and currents, both in theoretical predictions and in simulations.

III. COMPUTER CALCULATION

We have developed a computer program using the master equation to calculate the current in an electron pump circuit. To proceed with a practical calculation, we must limit the number of states considered as well as the number of transitions. We must limit the state space to a finite number of number of electrons per island, say M_- to M_+, which reduces the number of states considered to $(N-1)^{(M_+-M_-+1)}$ states. We show in Appendix A that it is possible to verify that the size of the state space is sufficient.

The numerical problem is further reduced by limiting the number of tunneling configurations for the transitions between states. To do this, we will limit the order of perturbation theory by not considering second-order processes in a single junction, that is, processes that transfer two electrons simultaneously through the same junction. We can eliminate these types of processes because they are energetically favorable only at bias conditions very far from those to be considered for the pump circuit. This limits the order of perturbation theory to N and the number of tunneling configurations to 3^N-1.

A further reduction, which may be adequate for some applications, is obtained by considering only tunneling configurations in which all electrons tunnel in the same direction. This reduces the number of configurations to 2^{N+1}.

To integrate the master equation, Eq. (6), we must calculate the transition rate matrix. This is done systematically by considering all possible tunneling sequences from all possible initial states in the chosen state space. The number of such sequences is determined by the number of tunneling configurations, multiplied by the number of possible permutations for each configuration. The number of tunneling configurations is determined by the number of combinations of participating junctions and directions of tunneling.

From an initial state n_i we calculate all the possible tunneling sequences. Given a tunneling sequence $(j_1, j_2, ...)$ we then calculate the Coulomb energies for each of the intermediate states in the sequence $(\Delta E_1, \Delta E_2, ...)$ as described in Sec. II D. If one of these energies, say ΔE_k, becomes less than zero the sequence is broken off, because the rates for all higher-order tunneling processes vanish in the approximation used here. Hence, ΔE_k becomes the final energy for the process of order k. We may then determine the final state n_f from the new distribution of electrons and calculate the matrix element for this sequence $s(j_1, j_2, ..., j_k)$ from the intermediate energies $\varepsilon_1, ..., \varepsilon_{k-1}$, Eq. (13). We then add $s(j_1, j_2, ..., j_k)$ to S for the configuration $\{j_1, j_2, ..., j_k\}$. When all possible sequences have been calculated, we have then summed over all possible permutations of the configuration. The rate is then calculated from the square of S, the order k of the process, and the total change in energy ΔE_k. We then compute $\Gamma_{n_i n_f}$ from the sum of the rates over all configurations that take state n_i to state n_f.

The currents through the junctions are calculated from the transition rates by keeping track of the transitions, their direction, and which junctions they use. Consider, for example, the configuration $\{1, -2, 4\}$ corresponding to a third-order cotunneling event. The rate Γ' of this process depends on the initial state n. Given that the system is initially in state n, there is a current $e\Gamma'$ in junctions 1 and 4, and a current $-e\Gamma'$ in junction 2. We can thus keep track of the currents in N vectors $\gamma_1, ..., \gamma_N$, one for each junction, with the components of each vector indexed by the initial states. These vectors are calculated from the sum of the tunneling rates by the accounting described above. The total current is found by weighing the currents through the junctions by the probabilities of each of the initial states being occupied. The instantaneous current through junction i then becomes

$$I_i(t) = e\,\gamma_i(t) \cdot \mathbf{P}(t). \tag{18}$$

Details about algorithms and numerical techniques used in the program are given in Appendix A.

IV. ANALYTICAL PREDICTIONS

A. Array without charge biases

Although a computer program is able to calculate cotunneling currents for specific situations, we find it insightful to predict currents by analytical means. These predictions indicate in a general way what the optimal biasing conditions for a device should be. We consider the ideal pump circuit, Fig. 4, in which all junction capacitances are equal and the capacitance from the islands to ground are neglible, so the gate sources reduce to charge bias sources. Although this is a mathematical idealization of an experimental circuit, this symmetric circuit is useful because it allows a simple prediction for the accuracy. In a final design step, we can then use the computer program to predict the characteristics of a real junction circuit including all of the stray capacitance elements.

We first consider a linear array of N tunnel junctions with zero bias charge applied to each of the junction islands, as shown in Fig. 5(a). We are interested first in

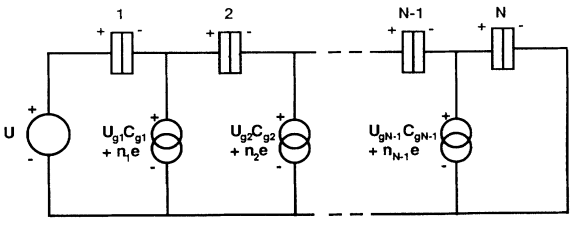

FIG. 4. Equivalent circuit of an idealized array of tunnel junctions with $C_{gi} \to 0$. The gate charge sources represent the induced charge $C_{gi}U_{gi}$ and the excess electrons n_i on the islands between the junctions. Also shown is the sign convention for charges and voltages.

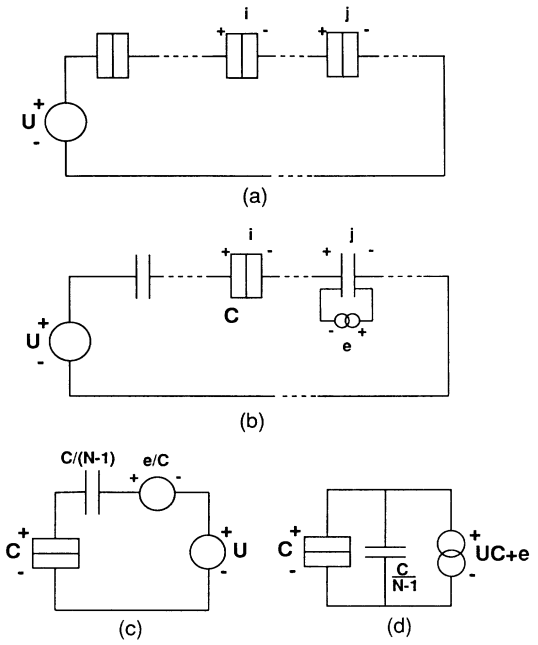

FIG. 5. The equivalent circuit reduction of a voltage biased array that already contains a tunneling event. Figure (a) is the circuit model of N tunnel junctions with capacitance C connected in series with a voltage source U, (b) the equivalent circuit for the junction labeled i in the case of junction j having already tunneled in the forward direction, (c) the circuit after using the Norton equivalent of a junction j as well as the series combination of the capacitances from the other junctions, and (d) the final Thevenin equivalent circuit which has an external charge $Q_x = (UC+e)/(N-1)$ and an external capacitance $C_x = C/(N-1)$.

finding an expression for the current-voltage characteristic. The cotunneling expression Eq. (16) requires the Coulomb energy after n junctions have tunneled. Here, as in the preceding section, we assume that a given junction tunnels only once in a cotunneling sequence. We first consider the Coulomb energy change when junction i tunnels, assuming that junction j has already tunneled, as shown in Fig. 5(b). The equivalent circuit in Fig. 5(c) is obtained by noting that an electron tunneling across the jth junction has as its Thevenin equivalent a voltage source e/C connected in series with that junction, which is then equivalent to a voltage across the entire array of $U + e/C$. Figure 5(c) also shows that the $N-1$ capacitors external to the ith junction are equivalent to a capacitance $C_x = C/(N-1)$. Figure 5(c) has its Norton equivalent to Fig. 5(d), from which the Coulomb energy change for a tunneling event in junction i can be calculated using Eq. (4) to be

$$\delta E_2 = \frac{e}{C+\frac{C}{N-1}}\left(\frac{e}{2} - (U+\frac{e}{C})\frac{C}{N-1}\right) = \frac{e}{NC}\left(e\frac{N-1}{2} - UC - e\right). \tag{19}$$

From the linearity of the circuit, we can also calculate the external charge of junction i when m other junctions have tunneled. The change in energy when junction i tunnels after m other junctions have already tunneled is

$$\delta E_{m+1} = \frac{e}{NC}\left(e\frac{N-1}{2} - UC - me\right). \tag{20}$$

Thus, the total Coulomb energy change after n junctions have tunneled is

$$\Delta E_n = \sum_{i=1}^{n} \delta E_i = \frac{e}{NC} n\left(e\frac{N-n}{2} - UC\right). \tag{21}$$

The total energy change ΔE_n is independent of the order or index of which junctions have tunneled because of the symmetry of the circuit. This greatly simplifies the analytical predictions.

Equation (21) can the be used along with Eq. (16) to predict the cotunneling current. We calculate the transition rate from the state $n_0 = (0,0,...)$. The N-cotunneling of one electron tunneling through every junction gives a final state equal to the initial state. The total energy change, Eq. (21), becomes

$$\Delta E_N = -eU, \tag{22}$$

and the intermediate energies using the approximation of Eq. (13) are

$$\varepsilon_k = \Delta E_k - \frac{k}{N}\Delta E_N = \frac{e}{NC}k\left(e\frac{N-k}{2} - UC\right) + \frac{keU}{N} = \frac{e^2}{2NC}k(N-k). \tag{23}$$

Since there are N factorial tunneling sequences for a configuration of N junctions, and all give rise to the same intermediate energies, we can readily calculate S from Eq. (10)

$$S = \sum_{\text{perm}} \prod_{k=1}^{N-1} \frac{1}{\varepsilon_k} = \left(\frac{2NC}{e^2}\right)^{N-1} N! \frac{1}{(N-1)!(N-1)!} = \left(\frac{2NC}{e^2}\right)^{N-1} \frac{N}{(N-1)!}. \tag{24}$$

Because the state n_0 is the only occupied state in this calculation, the current from this transition is $I_+ = e\Gamma_{n_0 n_0}$ with $\Gamma_{n_0 n_0}$ calculated from Eq. (16). The current is then given by

$$I_+ = \frac{N^{2N+1}}{\pi^{2(N-1)}[(N-1)!]^2(2N-1)!N}\left(\frac{R_K}{R_T}\right)^N \times \left(\frac{UC}{e}\right)^{2N-1} \frac{e}{R_K C}\mathcal{F}_N(t), \tag{25}$$

where we have defined the normalized version of F_n by

$$\mathcal{F}_n(t) \equiv \frac{F_n(\Delta E_n, T)}{(-\Delta E_n)^{2n-1}}(2n-1)! \tag{26}$$

with $t = k_B T/\Delta E_n$. At zero temperature, $\mathcal{F}_n$ reduces to the step function $\Theta(-\Delta E_n)$, cf. Eq. (15).

Equation (26) is equal to Eq. (28) in Ref. 9, because in the approximation used here, Eq. (13), the intermediate energies become independent of the bias voltage, and hence equivalent to using the low voltage limit in the quoted equation. Our expression for the intermediate energies is hence a justification for the use of Eq. (28) in Ref. 9 also for finite voltages.

However, cotunneling of orders less than N can occur at large enough finite voltages. From Eq. (14), a cotunneling process of order m occurs when the energy ΔE_m is less than or equal to zero at zero temperature. Equation (21) shows that $\Delta E_m \leq 0$ when

$$\frac{UC}{e} \geq \frac{N-m}{2}. \tag{27}$$

Thus, as the voltage increases, lower-order cotunneling processes are allowed. Within our approximation, the higher-order cotunneling simultanously vanishes. When cotunneling with order $m < N$ occurs, the system makes transitions to final states different from the initial state $n_0 = (0, 0, ...)$. We find from computer solutions of the full master equation that after the m-order cotunneling events, the system makes a series of complicated secondary transitions to many other states through 1-junction to $(N-m)$-junction cotunneling transitions, but eventually makes a transition to the state n_0. In this case, the secondary transitions bring the system back to the initial state by electrons tunneling in the same direction as in the initial m-order cotunneling process. The rates of the secondary processes, weighted by the occupation probability of their initial states, are much faster than the initial process. Therefore, the initial m-order cotunneling rate predicts the total current through the device. Since there are $\binom{N}{m}$ possible configurations of m junctions tunneling out of the $(0, 0, ...)$ state and all configurations give rise to the same rate, the current for these transitions is

$$I_+ = e\binom{N}{m}\Gamma^{(m)}, \tag{28}$$

where $\Gamma^{(m)}$ is the m-order cotunneling rate

$$\Gamma^{(m)} = \frac{m^{2m+1}}{\pi^{2(m-1)}[(m-1)!]^2(2m-1)!N}\frac{(R_K/R_T)^m}{R_K C} \times \left(\frac{UC}{e} - \frac{N-m}{2}\right)^{2m-1}\mathcal{F}_m(t). \tag{29}$$

In Fig. 6 we plot the zero-temperature prediction of Eq. (28) for a pump with five junctions along with the results of the computer program for parameters $R_T = 20R_K$ and $C_g = 10^{-5}C$. The calculated values and the result of Eq. (28) are in excellent agreement, with the worst agreement occurring for the lowest-order processes. The difference is due to the time spent in relaxing after low-order cotunneling processes, as well as the effect

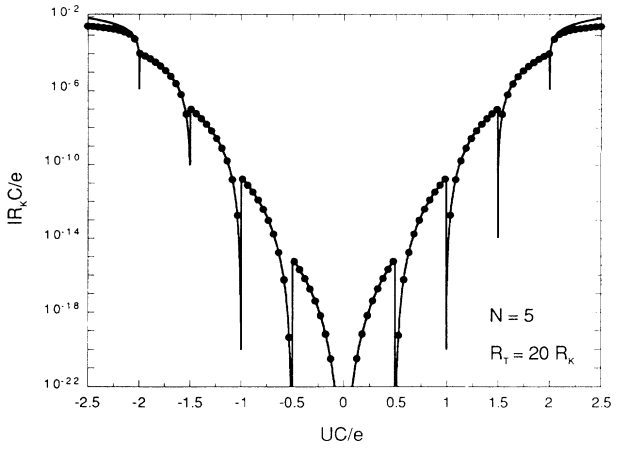

FIG. 6. Current-voltage characteristic of the voltage biased array without gate charge biases. The solid lines are the predictions from Eq. (28) and the points are from the full computer simulation. The parameters are $R_T = 20R_K$, $C_g = 10^{-5}C$ and $T = 0$.

of the finite gate capacitances. The discontinuities arise from the Θ function approximation in Eq. (17).

This comparison shows that it is possible to calculate the current by simply considering errors from ideal behavior; that is, only the current due to the unwanted processes. This approximation works because the details about how the system relaxes from excited states induced by cotunneling is unimportant. We therefore use this approach to calculate the current in the full pump circuit. The results from the full calculation in the computer program can then be used to validate this approach by comparison.

B. Array with gate sources

The circuit we consider is shown in Fig. 2. A series array of N small junctions is connected to a bias voltage source U. Each island between two junctions has a gate voltage source which is connected through a gate capacitor. We simplify the circuit by considering gate capacitances much smaller than the junction capacitances; hence, each gate source reduces to a charge source of magnitude $C_{gi}U_{gi}$. Furthermore, we assume that all junction capacitances and resistances are equal and given by C and R_T. The resulting circuit is shown in Fig. 4, as well as the sign conventions for charges and voltages. We call the direction of tunneling "forward" toward the grounded side of the circuit and "reverse" toward the bias source, and we symbolize the event of junction j tunneling in the forward or reverse direction by $\pm j$. Furthermore, we perform the calculations using positive units of charge.

We derive the equivalent external charge for a junction by first calculating the contribution from island i, which from Fig. 4 has a total charge bias of $\tilde{Q}_i = n_i e + Q_i$. Here $Q_i = U_{gi}C_{gi}$ is the gate charge bias and n_i is the number of electrons on island i. From the reduction shown in Figs. 7(a)–7(c) we calculate that

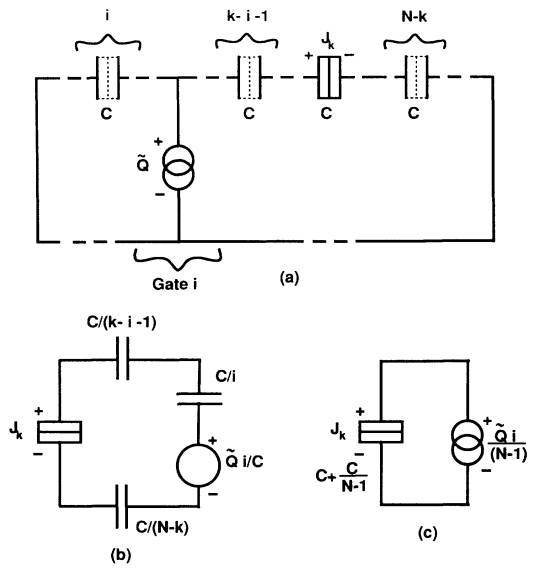

FIG. 7. Equivalent circuit used to calculate the contribution of a gate charge $\tilde{Q}$ to the external charge on junction k. Figure (a) is the circuit, (b) the circuit after using the Norton equivalent of the charge source in parallel with a capacitance, and (c) the final reduction to a circuit equivalent to Fig. 1(c).

the charge $\tilde{Q}_i$ contributes $\tilde{Q}_i\ i/(N-1)$ to the external charge Q_{xk} of junction k for $k > i$; for $k \leq i$, we find $\tilde{Q}_i\ (i-N)/(N-1)$. Similarly, we find that the bias voltage contributes $UC/(N-1)$ to the external charge of all junctions. The external capacitance for all junctions is given by $C_x = C/(N-1)$. Hence, the full expression for the external charge of junction j is

$$Q_{xj} = \frac{1}{N-1}\left(\underbrace{\sum_{i=1}^{j-1} i(Q_i + en_i)}_{j>1} + \underbrace{\sum_{i=j}^{N-1}(i-N)(Q_i+en_i)}_{j<N} + UC\right). \tag{30}$$

The underbraces indicate that the first sum does not apply to junction 1 and the second sum does not apply to junction N.

The external capacitance and charge is then used with Eq. (4) to calculate the change in energy due to a tunneling event in junction j in the forward or reverse direction

$$\delta E^{\pm j} = \frac{e^2(N-1)}{2NC}\left(1 \mp 2\frac{Q_{xj}}{e}\right). \tag{31}$$

An important special case is illustrated in Fig. 8. An antisymmetric bias charge is applied to the island around junction j, with $+\tilde{Q}$ on island $j-1$ and $-\tilde{Q}$ on island j. This bias configuration is equivalent to a charge bias around junction j, also shown in Fig. 8. The contribution to external charges is then easily shown to be

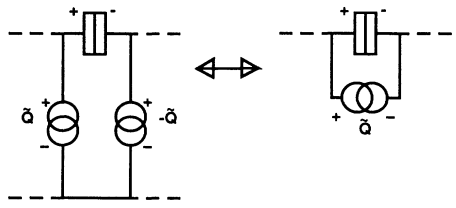

FIG. 8. The equivalence of an antisymmetric charge bias to a charge bias directly across a junction.

$$Q_{xi} = \frac{-\tilde{Q}}{N-1}, \quad i \neq j, \tag{32a}$$

$$Q_{xj} = \tilde{Q}, \tag{32b}$$

where the contributions are independent of the position in the array of both i and j. Hence, biasing junction j will also bias all the other junctions, but with a magnitude reduced by a factor of $-1/(N-1)$.

A junction tunneling event is equivalent to a charge bias of magnitude e around that junction. Therefore, the effect of tunneling is given by Eqs. (32a) and (32b) with $\tilde{Q}$ replaced by $-e$ for a forward transition and by $+e$ for a reverse transition. Because the tunneling of a junction changes the external charge in the other junctions independently of their position in the array, the calculation of Coulomb energies for an arbitrary cotunneling sequence is not difficult.

V. THE ELECTRON PUMP

Figure 2 shows an equivalent circuit of the electron pump. As illustrated in Fig. 9, the pump is biased so that a series of pulses to the island gates cause single electrons to sequentially tunnel through the junctions. We will first discuss some of the conditions for optimal bias and argue that the pulsed biasing scheme shown in Fig. 9 meets these conditions. We will derive the optimal bias for the voltage across the pump U equal to zero and assume that the optimal biasing changes little for finite U.

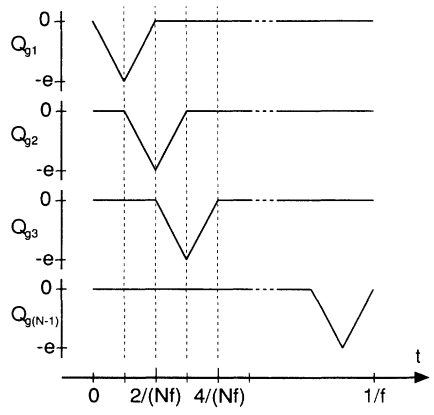

FIG. 9. Time dependence of gate voltages for the electron pump. The operating frequency is f. The gate voltages satisfy the optimal gate biasing $Q_j + Q_{j+1} + e = 0$.

We break the gate sequence into N parts. The jth part of the sequence will transfer an electron through junction j, from island $j-1$ to island j. We call junction j the biased junction and all the other junctions unbiased.

A. Optimal biasing

At the beginning and end of a part of the gate sequence, we want the electron to be optimally stable on islands $j-1$ and j. The most stable bias configuration is obtained when $\Delta E_1^{\pm}$ is maximum, or $Q_{xi}=0$ for all junctions. At the beginning, this bias configuration is obtained by setting the gate charge $Q_{j-1}=-e$ and $Q_i=0$ for $i\neq j$. At gate $j-1$ the total charge is $Q_{\rm tot}=Q_{j-1}+e=0$, as is the charge on all other islands, thus satisfying $Q_{xi}=0$ for all i. At the end of this part of the gate sequence, the electron is on island j. If $Q_j=-e$ and all other gate charges are equal zero, we again have the maximally stable state. The question of optimal bias now reduces to how the bias charges are changed from the beginning to the end of this part of the sequence.

Equation (32a) predicts that when a cotunneling event occurs, the external charge on all the unbiased junctions changes by $e/(N-1)$. Because the tunneling event is stochastic, we cannot obtain $Q_{xi}=0$ for the unbiased junctions both before and after the tunneling. The most stable situation is to have the external charges of the unbiased junctions change from $Q_{xi}=-\frac{1}{2}e/(N-1)$ to $\frac{1}{2}e/(N-1)$ when the biased junction tunnels, which will occur near $Q_{xj}=e/2$. This situation can be accomplished by setting $Q_{j-1}=Q(t)-e$ and $Q_j=-Q(t)$, where $Q(t)$ varies from 0 to e from the beginning to end of the part of the gate sequence, and all other gate charges equal zero. This biasing gives $Q_{j-1}+Q_j=-e$. If $Q_{j-1}+Q_j$ is different from $-e$, say $-e+Q'$, there will be an additional shift of Q_x of the unbiased junctions coming from Q', which moves the system away from best biasing [see Eq. (30)].

The operation of the pump is thus equivalent to the antisymmetric biasing depicted in Fig. 8. When Q is varied from 0 to e, a tunneling event occurs in the biased junction and an electron is transferred from island $j-1$ to island j. This tunneling event is equivalent to a change in the charge bias $Q(t)\rightarrow Q(t)-e$. Because only antisymmetric bias configurations need be considered, only Eqs. (32a) and (32b) are needed to compute Q_x.

The derivation above is independent of which part of the gate sequence we considered. We need only to calculate the error current for one part of the sequence and then multiply by N to get the total error.

The sequence of triangular wave pulses shown in Fig. 9 is experimentally easy to implement and near optimal. We think that other waveforms which satisfy the condition $Q_{j-1}+Q_j+e=0$ can further improve the operation of the pump.

B. Single-junction tunneling

The biasing scheme derived above has simplified the gate biasing so that only the single variable Q need be considered. The junction bias voltage U then maps the complete biasing of the device to the two-dimensional space of Q and U. We now compute thresholds and rates for all processes similar to what was done in Sec. IV A. However, since Q contributes differently to the biased and the unbiased junctions, we must consider the tunneling in each of these two junction types separately.

With a charge bias Q placed across the biased junction j and a voltage U applied to the entire array, the external charges are

$$Q_{xi}=\frac{-Q+UC}{N-1},\quad i\neq j, \tag{33a}$$

$$Q_{xj}=Q+\frac{UC}{N-1}. \tag{33b}$$

We compute the region in the Q-U plane for which the system is stable with respect to single-junction transitions; stable means in this context that single-junction tunneling events are energetically unfavorable. This is found by requiring that $-e/2<Q_x<e/2$ for all Q_x. Hence from Eqs. (33a) and (32b) we obtain the conditions for Q and U in which no tunneling can occur for the biased and unbiased junctions respectively

$$Q-e\frac{N-1}{2}<UC<Q+e\frac{N-1}{2}, \tag{34a}$$

$$(1-N)Q-e\frac{N-1}{2}<UC<(1-N)Q+e\frac{N-1}{2}. \tag{34b}$$

These equations give the conditions before the biased junction has tunneled. After tunneling, the conditions are found by replacing Q with $Q-e$ in Eqs. (34a) and (34b), as explained in Sec. V A.

Because the tunneling of the biased junction can be described by a shift in Q of $-e$, we think that the conditions for tunneling are best described graphically as shown in Fig. 10, where we have solved Eqs. (34a) and (34b) for values of Q between $-e$ and e. Before the biased junction tunnels, the right origin of the Q axis is used. After the biased junction tunnels, Q is shifted by $-e$ and the left origin of the Q axis is used. The lines labeled $\pm j$ represent the threshold for an electron tunneling through the biased junction, one line for each direction. The lines labeled $\pm i$ similarly give the thresholds for any of the unbiased junctions. The solid lines indicate threshold lines before the biased junction has tunneled, the dashed lines after tunneling. The shaded area represents the stability region where it is energetically unfavorable for an electron to tunnel through any single junction.

Because the pump is used with a constant voltage U, the operation of the device is then described by a trajectory in the Q-U plane of a line parallel to the Q axis. The trajectory starts at $Q=0$ on the U axis and moves to the right. When the biased junction tunnels, the trajectory jumps by the amount e to the left. The trajectory ends at $Q=e$, which is again on the U axis.

We see that at $U=0$, the threshold for tunneling for the biased junction is $Q=\pm e/2$. The value of this threshold changes with U. The threshold lines of $+j$ and $-j$ are displaced from each other in Q by e, as expected.

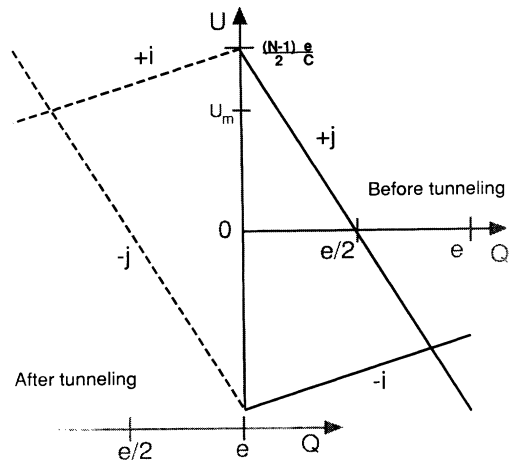

FIG. 10. Threshold lines for single-junction tunneling with gate bias Q and voltage bias U. The origin of the Q axis shifts by $-e$ when the biased junction tunnels; the threshold lines are correspondingly solid and dashed. The threshold lines for the biased junction are labeled $\pm j$, and for the unbiased junctions $\pm i$. The stability region for single-junction tunneling is shaded.

Errors in the pump cycle occur when the trajectory enters a region where unbiased junction transitions are possible. This happens when $|U| > U_m = (e/C)(2N^2 - 3N + 2)/2N$.

C. Decay of initial state

Because the biased junction does not switch immediately upon crossing its threshold, errors in the pumping of electrons may arise from operating the device at too high a frequency. We calculate this error for the triangular gate voltages which are depicted in Fig. 9.

At zero temperature, the biased junction j tunnels after it reaches its threshold. The change of energy and the rate for tunneling are

$$\Delta E = -\frac{e(N-1)}{NC}\left(Q - \frac{e}{2} + \frac{UC}{N-1}\right), \tag{35}$$

$$\Gamma^{(1)} = \frac{-\Delta E}{e^2 R_T} = \frac{N-1}{eNR_TC}\left(Q - \frac{e}{2} + \frac{UC}{N-1}\right), \tag{36}$$

where Q varies from the threshold value $e/2 - UC/(N-1)$ to e. The probability of remaining in the initial state satisfies the rate equation

$$\frac{dP}{dt} = -\Gamma(t)P(t), \quad P(0) = 1. \tag{37}$$

The pump cycle of Fig. 9 gives $dQ/dt = eNf$, where f is the pumping frequency. We introduce $\Delta Q = Q - e/2 + UC/(N-1)$ as the distance in Q from the threshold line, and integrate Eq. (37) to obtain

$$\begin{aligned} P(t) &= \exp\left(-\int_0^t \Gamma(\tau)d\tau\right) \\ &= \exp\left(-\int_0^{\Delta Q} \frac{N-1}{eNCR_T}\frac{qdq}{eNf}\right) \\ &= \exp\left[-\frac{N-1}{2N^2}\frac{1}{R_TCf}\left(\frac{\Delta Q}{e}\right)^2\right]. \end{aligned} \tag{38}$$

We consider here that an error occurs if junction j has not tunneled when Q reaches the final value e; Appendix B discusses this situation in more detail. As will be shown in the next section, cotunneling contributes to the errors before Q reaches e. The probability of not having switched when reaching $Q = e$ is

$$P = \exp\left[-\frac{N-1}{2N^2R_TCf}\left(\frac{1}{2} + \frac{UC}{e(N-1)}\right)^2\right] \tag{39}$$

which for $U = 0$ is equal to the result in Sec. 5.2.3.2 of Ref. 10. The error rate of the pump increases exponentially with frequency.

D. Cotunneling

The cotunneling calculation is simplified because all the unbiased junctions behave equivalently. Thus, the N junctions of the array can be grouped into two classes, the biased junction and the unbiased junctions. We then can group cotunneling processes by class and direction.

We will not consider processes where more than one electron tunnels simultaneously through the same junction. Nor will we include processes involving n unbiased junctions tunneling in one direction together with m unbiased junctions in the opposite direction. The biasing conditions of these processes are found to occur only at extreme values of the biasing parameters $|Q - UC| > (N-1)e$. Thus, they are not important.

First we compute when cotunneling of order n can occur. The final energy, which depends only on which junctions are tunneling, must thus be less than zero. We can break the types of processes into six distinct groups: $\{+, +(n-1)\}$, $\{-, +(n-1)\}$, $\{+, -(n-1)\}$, $\{-, -(n-1)\}$, $\{0, +(n)\}$, and $\{0, -(n)\}$. Here we have labeled the direction of the processes by the sign of the tunneling event. The first entry represents the biased junction, the second represents the number of unbiased junctions, and zero symbolizes that the junction does not participate.

We first consider the four types of processes in which all junctions tunnel in the same direction. We calculate the change in energy δE_k for the kth tunneling event $\pm j_k$ after the sequence $(j_1, j_2, ..., j_{k-1})$. Since a tunneling event in any junction, biased or unbiased, results in a change in the external charge of magnitude $e/(N-1)$ in all other junctions, the contribution to the external charge after $k-1$ tunneling events is $e(k-1)/(N-1)$ to the kth junction. Using Eqs. (31), (33a), and (33b), we find

$$\delta E_k^{\pm j_k} = \frac{e^2}{2NC}\left[N - 1 \mp 2\left(\frac{-Q + UC}{e} \pm (k-1)\right)\right],$$

unbiased junction, (40a)

$$\delta E_k^{\pm j_k} = \frac{e^2}{2NC}\left[N-1\mp 2\left(\frac{(N-1)Q+UC}{e} \pm(k-1)\right)\right],$$

biased junction. (40b)

Because the final Coulomb energy is independent of the sequence of tunneling events, the final energy ΔE_n is the sum of the individual changes given in Eqs. (40a) and (40b). For example, in the case of a tunneling configuration of n unbiased junctions tunneling in the forward direction, the $\{0,+n\}$ process, we find

$$\Delta E_n = \sum_{k=1}^{n} \delta E_k^{+j_k} = \frac{e^2 n}{NC}\left(\frac{Q-UC}{e}+\frac{N-n}{2}\right). \quad (41)$$

This process occurs when $\Delta E_n < 0$, which gives

$$U\frac{C}{e} > \left[\frac{Q}{e}+\frac{N-n}{2}\right]. \quad (42)$$

This defines a threshold line for the $\{0,+(n)\}$ cotunnneling process, similar to those found in Sec. V B for the single-junction tunneling events. Similar results are found in this manner for the other three cotunneling processes, $\{0,-(n)\}$, $\{+,+(n-1)\}$, and $\{-,-(n-1)\}$.

In the case of mixed-direction processes, $\{+,-(n-1)\}$ and $\{-,+(n-1)\}$, we obtain

$$\delta E_1^{\pm j_1} = \frac{e^2}{2NC}\left[N-1\mp 2\left(\frac{(N-1)Q+UC}{e}\right)\right], \quad j_1 = \text{biased}, \quad (43)$$

$$\delta E_k^{\mp j_k} = \frac{e^2}{2NC}\left[N-1\pm 2\left(\frac{-Q+UC}{e}\pm 1\mp(k-2)\right)\right], \quad j_k \neq \text{biased}. \quad (44)$$

The change in Coulomb energy for n-order tunneling becomes

$$\Delta E_n = \frac{e^2}{2NC}\left[4\,(n-1)+n(N-n) \mp\left(\frac{(N+n-2)Q-(n-2)UC}{e}\right)\right]. \quad (45)$$

We find from Eq. (45) that these processes occur far from the bias region that is used when normally operating the electron pump. Thus these processes will not be considered further in this paper. In this way we have reduced the number of tunneling configurations that need to be considered to only 2^{N+1}.

Hence, for each order of cotunneling, only four threshold lines are important. These results are summarized in Table I.

Figure 11 shows the threshold lines in the Q–U plane for an N array. The labeling of the lines is placed on the side where the process is possible. The calculation above assumes an initial state where junction j is biased and the electron is on island $j-1$. However, the threshold lines are easily calculated for when the electron has tunneled by simply replacing Q with $Q-e$ in Eqs. (40a)–(45) and in Table I. As is shown in Fig. 10, we can therefore depict the Q biasing after tunneling with a shift in the origin of the Q axis.

There are regions in the biasing plane where several distinct types of processes are possible. For example, at the point labeled A in Fig. 11, tunneling through junction j and 2-cotunneling are both allowed, and hence compete. This possibility is important as it produces errors, and it will be explored below.

The graphical description of the biasing in Fig. 11 is extremely useful for predicting what voltages U give low error rates. Because error rates are lower for higher-order cotunneling processes, we want to operate in regions of the Q–U plane with the highest-order processes. As described in Sec. V B, the operation of the pump is given by the trajectory of a line parallel to the Q axis. The biased junction tunnels very close to the threshold line $\{1,0\}$ for small pump frequencies. Point P in Fig. 11 shows that at small positive voltages, there is only cotunneling of order N before the biased junction switches. However, after the biased junction switches, the bias is at point P' and cotunneling of order $N-1$ is possible. In contrast, at small negative voltages cotunneling of order $N-1$ occurs before the switching. Thus, it is not possible to avoid cotunneling of order $N-1$. If we require that at most cotunneling of order $N-1$ is allowed, the bias voltage is restricted to $|U| < (e/2C)(N-1)/N$.

TABLE I. Regions in the Q-U plane for the four dominant types of cotunneling errors. The number of junctions is N, the order of cotunneling is n, and the range of Q is 0 to e.

Process allowed	Type
$U > [(1-N/n)(Q/e)+(N-n)/2](e/C)$	$\{+,+(n-1)\}$
$U > [(Q/e)+(N-n)/2](e/C)$	$\{0,+(n)\}$
$U < [(1-N/n)(Q/e)-(N-n)/2](e/C)$	$\{-,-(n-1)\}$
$U < [(Q/e)-(N-n)/2](e/C)$	$\{0,-(n)\}$

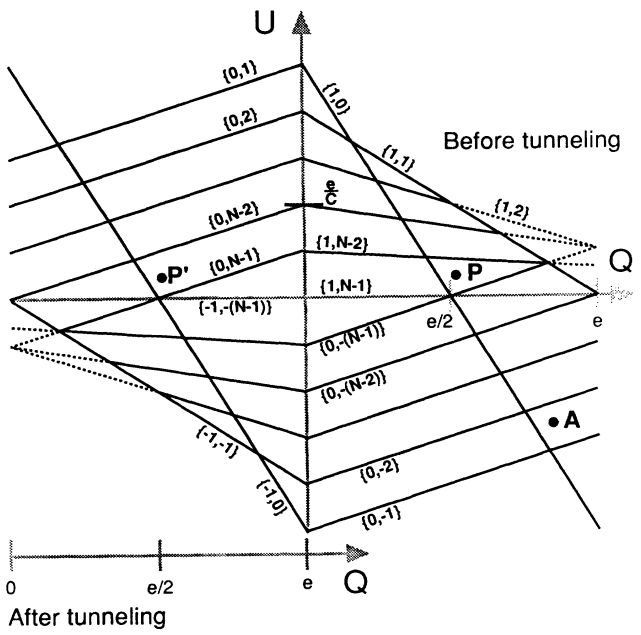

FIG. 11. Threshold lines for cotunneling, drawn similarly to Fig. 10. The lines are labeled with the type of process and are placed on the side of the threshold line where the process is allowed.

E. Cotunneling rates

We can calculate the cotunneling rates from the total change in energy and the intermediate energies. We first consider the cotunneling processes that involve only unbiased junctions, that is, processes of type $\{0,\pm n\}$. We define $|\Delta Q| = |Q - Q_T|$, where Q_T is the threshold value for the charge bias and ΔQ is positive above threshold. The total change in energy for the cotunneling event is

$$\Delta E_{\{0,\pm n\}} = -\frac{e}{NC} n \Delta Q. \tag{46}$$

The intermediate energies

$$\begin{aligned}\varepsilon_k &= \Delta E_{\{0,\pm k\}} - \frac{k}{n}\Delta E_{\{0,\pm n\}} \\ &= -\frac{e}{NC}k\left(\Delta Q - e\frac{n}{2} + e\frac{k}{2}\right) + \frac{k}{n}\frac{e}{NC}n\Delta Q \\ &= \frac{e^2}{2NC}k(n-k)\end{aligned} \tag{47}$$

do not depend on ΔQ and are the same as Eq. (23). These energies are used in Eq. (17), and noting that all permutations give rise to the same intermediate energies, we find

$$S = \left(\frac{2NC}{e^2}\right)^{n-1} \frac{n}{(n-1)!}. \tag{48}$$

The rate for the process as predicted from Eq. (16) is

$$\begin{aligned}\Gamma_{\{0,\pm n\}} &= \frac{n^{2n+1}}{\pi^{2(n-1)}[(n-1)!]^2(2n-1)!N} \\ &\quad \times \frac{[R_K/R_T]^n}{R_K C}\left(\frac{\Delta Q}{e}\right)^{2n-1} \mathcal{F}_n(t).\end{aligned} \tag{49}$$

In a similar fashion we derive the cotunneling rates for processes which involve the biased junction. However, now the intermediate energies will depend on the permutation of the tunneling configuration. A process of order n has sequences with n possible positions of the biased junction. The total change in energy is

$$\begin{aligned}\Delta E_n &= \Delta E_{\{\pm,\pm(n-1)\}} \\ &= \pm\frac{e}{NC} n\left(\left[1 - \frac{N}{n}\right]Q - UC \pm e\frac{N-n}{2}\right).\end{aligned} \tag{50}$$

If we again define ΔQ as the distance in Q above the threshold, we find

$$\Delta E_n = -\frac{e}{NC}(N-n)\Delta Q. \tag{51}$$

The Coulomb energy of the kth intermediate state depends on whether the biased junction has tunneled. For the two cases we find

$$\Delta E_k = \begin{cases} \Delta E_{\{\pm,\pm(k-1)\}} = \pm\frac{e}{NC}k\{[1-\frac{N}{k}]Q - UC \\ \qquad\qquad \pm\frac{e}{2}(N-k)\}, \\ \Delta E_{\{0,\pm k\}} = \pm\frac{e}{NC}k[Q - UC \pm \frac{e}{2}(N-k)], \end{cases} \tag{52}$$

and the intermediate energies are

$$\varepsilon_k = \begin{cases} \frac{e}{NC}k\left(e^{\frac{n-k}{2}} + NQ\frac{1}{n}\right), \\ \frac{e}{NC}k\left(e^{\frac{n-k}{2}} + NQ\left[\frac{1}{n} - \frac{1}{k}\right]\right). \end{cases} \tag{53}$$

We calculate the contribution to S for a process of order n and for the biased junction in the ith position. We sum over all the permutations of the unbiased junctions and find

$$\begin{aligned}\delta S &= \left(\frac{NC}{e}\right)^{n-1}\left(\prod_{k=1}^{i-1}\frac{1}{e^{\frac{n-k}{2}} + NQ\frac{1}{n}}\right) \\ &\quad \times \left(\prod_{k=i}^{n-1}\frac{1}{e^{\frac{n-k}{2}} + NQ\left[\frac{1}{n} - \frac{1}{k}\right]}\right).\end{aligned} \tag{54}$$

We must also sum over i, but only the terms that have positive Coulomb energy of the intermediate states [Eq. (52)]. Hence the expression for S becomes

$$S = \sum_{i:\Delta E_i > 0}^{n} \delta S. \tag{55}$$

The expression for the rate is

$$\begin{aligned}\Gamma_{\{\pm,\pm(n-1)\}} &= [\tilde{S}(Q/e)]^2 \frac{n^{2n+1}}{\pi^{2(n-1)}[(n-1)!]^2(2n-1)!N} \\ &\quad \times \frac{[R_K/R_T]^n}{R_K C}\left(\frac{\Delta Q}{e}\right)^{2n-1} \mathcal{F}_n(t),\end{aligned} \tag{56}$$

with

$$\tilde{S}(q) = \frac{(n-1)!}{n} \sum_{i:\Delta E_i>0}^{n} \left(\underbrace{\prod_{k=1}^{i-1} \frac{1}{n-k+\frac{1}{n}2Nq}}_{i>1} \right) \times \left(\underbrace{\prod_{k=i}^{n-1} \frac{1}{n-k+\left(\frac{1}{n}-\frac{1}{k}\right)2Nq}}_{i<n} \right). \quad (57)$$

F. Leakage and switching errors

We name cotunneling processes that occur inside the stability region (the shaded region in Fig. 11) "leakage errors," and those that occur outside "switching errors." The distinction is important because relaxation processes can cancel the switching errors, and the sign of the error current depends on the type of process.

The state of the pump is stable with respect to single-junction transitions inside the stability region. However, cotunneling causes transitions out of that state, which then lead to other transitions that eventually return the system back to the initial state. We will name these error processes "leakage errors." The net result of this error process is to transfer an electron through the entire array.

The biasing must eventually move Q outside the stability region so that the biased junction can tunnel. However, a competition then exists between the desired process and cotunneling, both of which result in an electron being transferred to the next island. Cotunneling most often causes an extra electron to transfer through the entire array, so an error is produced. These paths which switch to the new state through cotunneling and not through the tunneling of the biased junction will be named "switching errors."

Leakage errors cause the system to relax to the initial state by a combination of normal tunneling and cotunneling events. The direction of the relaxation is the same as the initial leak due to energy considerations. As in Sec. IV A, relaxation is fast compared to the initial cotunneling, so the current is given by the rate of the initial cotunneling. The error current is $\pm N_{\rm ch} e \Gamma_{\rm leak}(Q,U)$, where the number of channels $N_{\rm ch}$ is the number of possible combinations of unbiased junctions that participate. Hence, $N_{\rm ch} = \binom{N-1}{n}$ for processes $\{0, \pm n\}$, and $N_{\rm ch} = \binom{N-1}{n-1}$ for processes $\{\pm, \pm(n-1)\}$. A charge error of $\pm N_{\rm ch} e \Gamma_{\rm leak}\, dt$ will occur in a time dt, where the sign is given by the direction of the cotunneling.

Switching errors must also consider how the system relaxes to the new state with the electron on the next island. Two types of cotunneling errors can compete with the wanted transition $\{1,0\}$ of Fig. 11. One type $\{0,-n\}$ involves only unbiased junctions and transfers electrons in the opposite direction with respect to the wanted transition. The second type $\{1,n-1\}$ involves the biased junction and gives the desired transition, but also brings extra electrons partly through the array. We derive in Appendix C that the relaxation may reset the partial error caused by the cotunneling. In a first approximation we will not consider the resetting processes, but assume for this type that it always produces an error.

VI. OPERATION OF AN N-JUNCTION PUMP

A. Cotunneling errors

We show in Fig. 12 the threshold lines of the N-junction pump for small U. We examine the operation of the pump in the voltage interval $-(N-2)/2N < UC/e < (N-2)/2N$ where at most cotunneling of order $N-1$ occurs. We again assume a triangular waveform for the gate voltages as shown in Fig. 9. The calculations carried out below can easily be generalized for an arbitrary waveform.

We first consider a positive voltage. The intersections of the trajectory of the charge bias with the threshold lines are labeled in Fig. 12. We list the main cotunneling errors.

A–B: Leakage of order N in the forward direction.

B–C: Leakage of order N in the forward direction weighted by the probability $P(t)$ that the electron has not switched.

C–: Switching error of order $N-1$ in the reverse direction weighted by the probability $P(t)$ that the electron has not switched.

B'–C': Leakage of order $N-1$ in the forward direction weighted by the probability $1-P(t)$ that the electron has switched.

C'–A: Leakage of order N in the forward direction again weighted by the probability $1-P(t)$ that the electron has switched.

The total error charge can be calculated by summing the error currents from the five error regions and multiplying by a factor of N to account for the total error for the N cycles

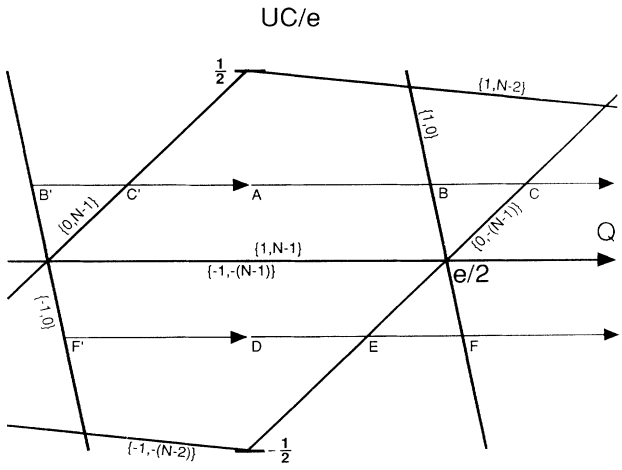

FIG. 12. The threshold lines of Fig. 11 around $U = 0$. Bias trajectories for the operation of the pump are lines parallel to the Q axis and are shown for positive and negative voltages.

$$Q_{+U} = Ne\Bigg(\int_A^B \Gamma_{\{1,N-1\}}dt + \int_B^C \Gamma_{\{1,N-1\}}P(t)dt - \int_C^1 \Gamma_{\{0,-(N-1)\}}P(t)dt + \int_{B'}^{C'} \Gamma_{\{0,N-1\}}[1-P(t)]dt + \int_{C'}^{A} \Gamma_{\{1,N-1\}}[1-P(t)]dt \Bigg). \quad (58)$$

We take $P(t)$ from Eq. (38), which uses only the dominant rate $\Gamma\{1,0\}$ for the decay of the initial state.

Similarly for negative voltages, we calculate the error charge

$$Q_{-U} = Ne\Bigg(-\int_D^E \Gamma_{\{-1,-(N-1)\}}dt - \int_E^F \Gamma_{\{0,-(N-1)\}}dt - \int_F^1 \Gamma_{\{0,-(N-1)\}}P(t)dt - \int_{F'}^{D} \Gamma_{\{-1,-(N-1)\}}[1-P(t)]dt \Bigg). \quad (59)$$

We first calculate the error charge for the dominant cotunneling processes of order $N-1$. We will show that the contribution from the terms of order N can be neglected.

The cotunneling rate of order $N-1$ is from Eq. (49)

$$\Gamma_{\{0,N-1\}} = K_{N-1}\frac{[R_K/R_T]^{N-1}}{R_K C}\left(\frac{\Delta Q}{e}\right)^{2N-3}, \quad (60)$$

where ΔQ is the distance from the threshold line and

$$K_{N-1} = \frac{(N-1)^{2N-1}}{\pi^{2N-4}[(N-2)!]^2(2N-3)!N}. \quad (61)$$

Table II numerically lists K_{N-1} for several values of N.

The fourth term in Eq. (58) contributes to the error charge by

$$Ne\int_0^{\tilde{u}} \Gamma_{\{0,N-1\}}(\tilde{u}-q)[1-P(q)]\frac{dq}{Nf}, \quad (62)$$

where $\tilde{u} = uN/(N-1)$, $u = UC/e$, $q = \{Q/e - [1/2 - u/(N-1)]\}$ is the normalized distance from the threshold of process $\{1,0\}$, and $P(q)$ is the probability that the electron has not tunneled. The integral can be expressed in terms of the error function, but in order to derive a simple expression, we will use for $P(q)$ a step function given by

TABLE II. Values of a_N and K_{N-1} used for calculating error rates.

N	K_{N-1}	a_N
4	1.169×10^{-2}	1×10^{-5}
5	3.006×10^{-4}	1×10^{-7}
6	4.103×10^{-6}	1×10^{-9}
7	3.466×10^{-8}	5×10^{-12}

$$P(q) = \begin{cases} 1, & q \le \langle q\rangle, \\ 0, & q > \langle q\rangle, \end{cases} \quad (63)$$

where $\langle q\rangle$ is an average switching distance defined by

$$\langle q\rangle = \int_0^\infty P(q)\frac{dq}{Nf} = \sqrt{\frac{N^2\pi R_T C f}{2(N-1)}}. \quad (64)$$

The third and fourth terms in Eq. (58) for cotunneling of order $N-1$ are mutually exclusive when using the step function for the probability function. We find the same magnitude for the error charge in the two cases, given by

$$Ne\frac{K_{N-1}}{2N(N-1)}\frac{(R_K/R_T)^{N-1}}{R_K C f}(\tilde{u}-\langle q\rangle)^{2N-2}. \quad (65)$$

The sign of the error, whether the error charge is transferred in the forward or the reverse direction, is given by the sign of $(\tilde{u}-\langle q\rangle)$.

For negative voltages we can evaluate the two integrals for processes of order $N-1$ in Eq. (59) exactly; the result is a polynomial in U of order $(N-1)^2$. In fact, this is also a good approximation of the error charge at positive voltages. However, the coefficients of the polynomial cannot be put in a simple form and must be evaluated for each N separately, and thus are not very useful. We again use the step function approximation for the probability $P(q)$ to find the error charge

$$Ne\int_0^{|\tilde{u}|+\langle q\rangle} \Gamma_{\{0,-(N-1)\}}\frac{dq}{Nf}, \quad (66)$$

which is evaluated to give the expression in Eq. (65).

Hence in the approximation used here, we find the total error due to cotunneling of order $(N-1)$ is

$$|Q_\varepsilon| = \frac{N^{2N-2}}{2\pi^{2N-4}[(N-2)!]^2(2N-3)!}\frac{(R_K/R_T)^{N-1}}{R_K C f} \times (u-q_0)^{2N-3}, \quad (67)$$

where $q_0 = \sqrt{(\pi/2)(N-1)R_T C f}$ and the sign of Q_ε equals the sign of $u-q_0$.

The cotunneling rate for cotunneling of order N is

$$\Gamma_{\{\pm1,\pm(N-1)\}} \propto \left(\prod_{k=1}^{N-1}\frac{1}{[k^2-(2Q/e)^2]}\right)^2\left(\frac{|U|C}{e}\right)^{2N-1}. \quad (68)$$

We approximate the rate by taking only the lowest power of Q into account, thus

$$\Gamma_{\{\pm1,\pm(N-1)\}} \approx a_N\frac{[R_K/R_T]^N}{R_K C}\left(\frac{|U|C}{e}\right)^{2N-1} \times \left(\frac{1}{4}-(Q/e)^2\right)^{-2}, \quad (69)$$

where a_N is found numerically and is given in Table II. The approximation is accurate within a factor of 2 over the range of Q. The maximum rate for cotunneling of order N occurs at the threshold for single-junction tunneling $\{1,0\}$, and gives $Q_{\max} = e/2 - |U|C/e(N-1)$.

The maximum rate for $UC/e \lesssim 0.3$ is

$$\Gamma_{\{1,N-1\}}|_{\max} \approx a_N \frac{[R_K/R_T]^N}{R_K C} \left(\frac{UC}{e}\right)^{2N-3} (N-1)^2. \tag{70}$$

We calculate a rough bound of the error charge from the process of order N by using the expression for the maximum rate times the period of the cycle. Hence the ratio of the error charge from cotunneling of order N, given by $Ne\,\Gamma_{\{1,N-1\}}|_{\max}$, to the error from cotunneling of order $N-1$, from Eq. (67), is approximately

$$\frac{Q_{\varepsilon,N}}{Q_{\varepsilon,N-1}} \lesssim \frac{a_N (N-1)^{2N+1}}{K_{N-1} N^{2N-2}} \frac{R_K}{R_T} u. \tag{71}$$

We can neglect the cotunneling processes of order N from the total error estimate, because its contribution to the total error is in general lower than the contribution from cotunneling of order $N-1$.

This estimate is also useful for understanding the effect of our approximation on the cotunneling rates at threshold, as discussed in Sec. II D. We expect an exact theory for cotunneling to have rates at threshold given approximately by Eq. (70) and to decay smoothly to zero above threshold. The region of Q in which we have to approximate the cotunneling rates has a length much smaller than e. Thus, Eq. (71) can be used to bound the error due to this approximation, and thus can be neglected when compared to errors of order $(N-1)$. Only because the bias point is changed continuously and the rates are averaged is the exact rate at threshold unimportant.

The integrals for cotunneling of order $(N-1)$ in Eqs. (58) and (59) can be expressed for the exact expression of $P(q)$ in terms of confluent hypergeometric functions and the error function. We plot in Fig. 13 that result, our estimate above from Eq. (67), and the output of our master equation-based simulation program for some reasonable system parameters. Equations (58) and (59) match the master equation very well, and cotunneling from order $(N-1)$ indeed predicts the errors well. The power law expression of Eq. (67), although simple, is a fair approximation especially for values of $|u-q_0| \gtrsim 0.1$.

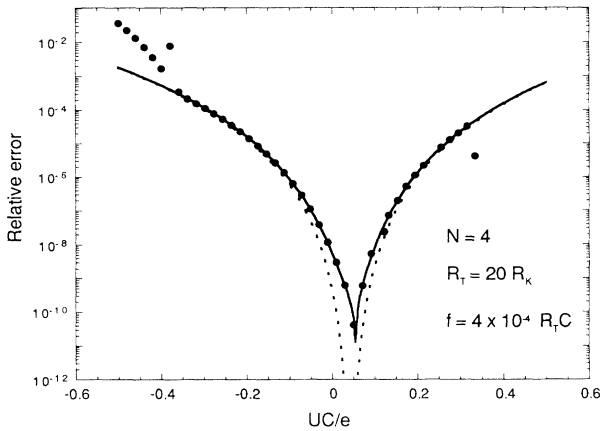

FIG. 13. The magnitude of the relative error from ideal pump operation versus bias voltage. Plotted are results from the computer simulation (dots), integration of the $N-1$ order terms in Eqs. (58) and (59) (solid line), and the simple formula of Eq. (67) (dashed line). System parameters are $N = 4$, $R_T = 20R_K$, $f = 4 \times 10^{-4}/R_T C$, and $T = 0$.

B. Thermal errors

We now calculate the effect of thermal fluctuations on the accuracy. First, we calculate the exponential factor which is the dominant factor of the error rate. Then we calculate the prefactor which gives the magnitude of the error.

We assume the thermal error rate is low so that we can calculate the transition rates away from ideal pump behavior, as was done for cotunneling. We make the approximation here that the temperature is high enough that the thermal error rate is higher than cotunneling rates, so we only need to consider single-junction tunneling. The expressions we derive are thus not necessarily valid in the region of crossover between thermal errors and cotunneling errors. However, the computer program can be used in this region to calculate the error rates.

Since thermally induced transitions of a single junction can reset themselves, a sequence of single-junction transitions must be considered. In fact, these sequences are exactly those described for cotunneling. The probability that a state in such a sequence is thermally occupied is $\exp(-\Delta E/kT)$, where ΔE is the energy difference between that state and the state corresponding to the ideal pump state. When more than one single-junction transition is needed to go to this state, ΔE is found by summing the energy differences of the single-junction transitions as was done in Eq. (8) for the cotunneling matrix element. The thermal error rate can be calculated from the process of thermal escape from a potential well, only here states that give the potential are discrete and given by the tunneling sequence. The thermal error rate for a particular sequence of single-junction tunneling events will thus be proportional to the Boltzmann factor $\exp(-\Delta E'/kT)$, where $\Delta E'$ is the maximum ΔE of that sequence. The total transition rate will be dominated by the sequence or sequences with the smallest $\Delta E'$, which we will denote as ΔE_m.

The expressions for the intermediate Coulomb energies are known from Sec. V D, where we calculate the intermediate energies for cotunneling. The lowest energy barriers ΔE_m occur for sequences that are the same as the cotunneling sequences of order $N-1$. If we assume for simplicity here that the biased-junction transition occurs at its threshold, the minimum ΔE_m will occur at points B' and F in Fig. 12. Equation (41) is used to calculate ΔE, with $q = -1/2 - u/(N-1)$ for the bias at B'. The maximum value of ΔE occurs for n junctions having tunneled with $n = (N-1)/2$ for N odd, and $n = N/2 - 1$ for N even. Equation (41) is used to find

$$\Delta E_m = E_c \left(\frac{(N-1)^2}{4N} - |u|\right), \quad N \text{ odd}, \tag{72}$$

$$\Delta E_m = E_c \left(\frac{N-2}{4} - |u|\frac{N-2}{N-1}\right), \quad N \text{ even}, \tag{73}$$

where $E_c = e^2/2C$. For $N = 4$, 5, 6, and 7 we compute

$$\Delta E_m = \begin{cases} \frac{1}{2} E_c \left(1 - \frac{4}{3}|u|\right), & N = 4, \\ \frac{4}{5} E_c \left(1 - \frac{5}{4}|u|\right), & N = 5, \\ E_c \left(1 - \frac{4}{5}|u|\right), & N = 6, \\ \frac{9}{7} E_c \left(1 - \frac{7}{9}|u|\right), & N = 7. \end{cases} \tag{74}$$

Larger junction arrays will produce smaller thermal errors at a fixed value of E_c/kT. The energy barrier ΔE_m does not decrease much at finite voltages as long as $|u| \lesssim 0.2$.

We calculate the prefactor to the thermal error rate by assuming that the temperature is low enough so that the occupation probability is $\exp(-\Delta E/kT)$ for all states except the state corresponding to ΔE_m at the top of the energy barrier. The occupation of this state is depleted because escape events over the top of the energy well never return. If Γ_+ and Γ_- are, respectively, the escape rates from the top state out of the well and back into the well, then the net escape from the well is

$$\Gamma = \frac{\Gamma_+ \Gamma_-}{\Gamma_+ + \Gamma_-} \exp(-\Delta E_m/kT). \tag{75}$$

Because there is only one state near maximum energy for N odd, but two states for N even, we must calculate the single-junction transition rates $\Gamma = \delta E/e^2 R_T$ separately for these two cases. The change in energy δE between the nth state and the $(n+1)$th state is $-E_c/N$ for N odd and $-2E_c|u|/(N-1)$ for N even. We have calculated this term to lowest order in u and at the threshold for the biased junction.

For N odd, the total error is given by summing the errors from C' to B'

$$|Q_\varepsilon| = eN_{ch} \frac{N-1}{2} N \frac{1}{2} \frac{(-\delta E)}{e^2 R_T} e^{-\Delta E_m/kT} \times \int_0^{q_t} \exp\left[-E_c \frac{N-1}{N} q/kT\right] \frac{dq}{Nf}, \tag{76}$$

where $N_{\rm ch} = \binom{N-1}{(N-1)/2}$ and accounts for the $N_{\rm ch}$ possible configurations of states with ΔE_m, $(N-1)/2$ accounts for the number of possible junction transitions out of this state, and the remaining N factor accounts for the N cycles for the pump. The exponential factor in the integral allows us to set the threshold charge q_t to infinity. We find

$$|Q_\varepsilon| = \frac{e}{8} \binom{N-1}{(N-1)/2} \frac{kT}{E_c} \frac{1}{R_T C f} \exp\left[-\Delta E_m/kT\right]. \tag{77}$$

For N even, we find with a similar calculation and for $u \gtrsim (kT/E_c)/2(N-1)$,

$$|Q_\varepsilon| = \frac{e}{2} \binom{N-1}{N/2-1} \frac{N^2}{(N-1)(N-2)} \frac{kT}{E_c} \frac{1}{R_T C f} \times |u| \exp\left[-\Delta E_m/kT\right]. \tag{78}$$

In Fig. 14 we have plotted the error versus $1/T$ for both a 4 pump and 5 pump together with the predictions of Eqs. (77) and (78). We see good agreement at high T between the errors found by our computer simulation and the simple formulas derived above. At low temperatures, cotunneling errors dominate.

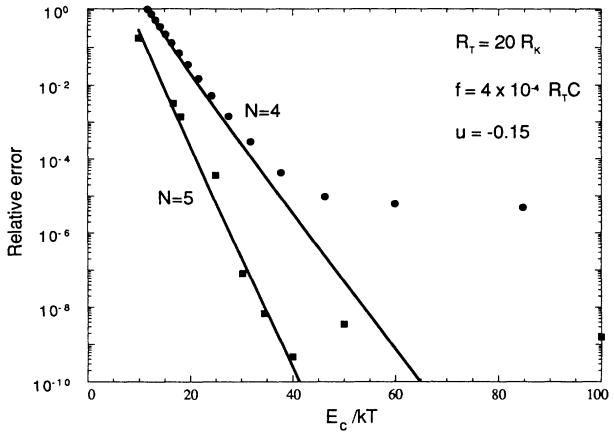

FIG. 14. Relative error versus inverse temperature for the computer simulation (points) and the predictions of Eqs. (77) and (78) (lines). Parameters are $N = 4$ (circles), 5 (squares), R_T=20 R_K, $f = 4 \times 10^{-4}/R_T C$, and $u = -0.15$.

C. Frequency errors

We found in Sec. VI A that the effect of frequency is to shift the voltage of minimum error to positive voltages. However, at high enough frequencies cotunneling of lower order can occur which then produces errors. Figure 11 shows that for negative voltages, $(N-2)$-order processes of type $\{0, -(N-2)\}$ can occur, while at positive voltages, the second-order process $\{1, 1\}$ can occur. We expect a significant increase in the error rates if these processes become active. We assume as a first approximation that an error occurs if the bias point crosses the threshold lines for one of these low-order processes. The error charge is thus given approximately by $eNP(t)$, where P' is the probability that the electron has not switched when reaching the threshold line for the lower-order process. For small voltages we therefore expect P' to be given by Eq. (38) with $\Delta Q \approx e/2$.

We have in Fig. 15 plotted the error charge for a 4 pump versus inverse frequency at $u = 0, \pm 0.1$. The figure shows a clear onset of the lower-order processes as an exponential increase in the error rate at higher frequencies. From the simulations we find an effective value of ΔQ that can be used in Eq. (38) to estimate the limitation on frequency. We find a value of $\Delta Q_{\rm eff} \approx 0.8e$ for $|U|C < 0.1e$. As a conservative estimate we will use $\Delta Q_{\rm eff} = 0.5e$ for subsequent calculations. We recommend using the computer simulation for larger voltage ranges or to estimate the maximum frequency to better than a factor of 2.

D. Summary of error processes

We have predicted the accuracy of the N-junction electron pump through three error sources: cotunneling [Eq.

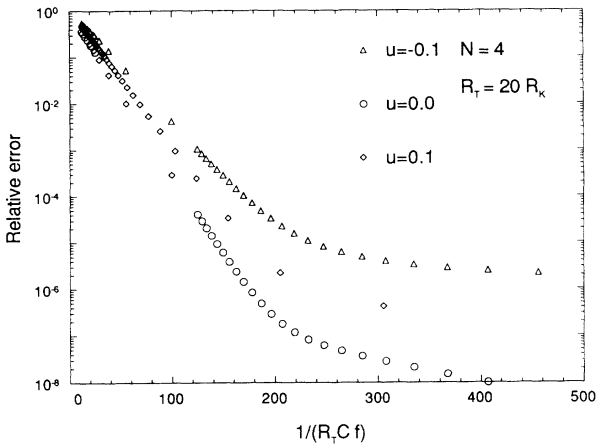

FIG. 15. Relative error versus inverse frequency obtained from the computer simulation. An increased error rate is seen at high frequencies. The slopes of the curves at high frequencies are used to calculate an effective ΔQ in Eq. (38). Parameters are $N = 4$, 5, $R_T = 20R_K$, and $T = 0$.

(67)], thermal [Eqs. (77) and (78)], and frequency (Sec. VI C). We summarize the results in this section in a way that allows the basic junction parameters to be determined given a desired accuracy.

Since we are typically interested in operating the pump as fast as possible, the constraints from $\mathcal{E}_f$ can be used to eliminate the variable f from the prefactors of the expressions for $\mathcal{E}_{\rm ct}$ and $\mathcal{E}_{\rm th}$. The dominant functional dependence of the errors can then be written as

$$\mathcal{E}_f = \exp\left[-\frac{a}{R_T C f}\right], \tag{79}$$

$$\mathcal{E}_{\rm ct} = b\,(R_K/R_T)^{N-2}\,|u-q_0|^{2N-2}, \tag{80}$$

$$\mathcal{E}_{\rm th} = c\,\exp\left[-d\,\frac{E_c}{kT}\right], \tag{81}$$

where each of the parameters a, b, c, and d depend on N, $|u|$, and the parameters themselves. We emphasize that these simple formulas are approximate and valid only when $0.1 \lesssim |u-q_0| \lesssim 0.4$. More exact expressions are found from the full formulas given in the previous sections.

We use Eq. (79) for $\mathcal{E}_f$ to determine R_TCf. We choose the desired voltage range $|u|$, and from $\mathcal{E}_{\rm ct}$ we find the necessary R_T. We then use $\mathcal{E}_{\rm th}$ to determine E_c/kT. From the experimental temperature and the value found for E_c/kT, we determine the necessary junction capacitance C. This value and R_T give the maximum frequency f.

Since we typically operate the pump at the maximum possible frequency, q_0 will in general be about 0.07. Since the exact value of q_0 is not known, a range of $|u-q_0| = 0.1$ is a reasonable minimum operating voltage range. We keep comfortably away from cotunneling of order $N-2$ by choosing a maximum range of $|u-q_0| = 0.3$. Finally, self-

TABLE III. Parameters needed to achieve error levels below 10^{-6} and 10^{-9}. We use $\Delta Q_{\rm eff} = 0.5$ for the frequency error. The parameters b, c, and d are given for the calculated value of R_TCf, and c is a self-consistent value of E_c/kT. An experimental temperature of 100 mK is used to compute the values of C and f

N	4		5		6		7	
$\lvert u-q_0\rvert$	0.1	0.3	0.1	0.3	0.1	0.3	0.1	0.3
				Error level 10^{-6}				
a	0.015		0.0128		0.0111		0.0098	
R_TCf	1.70×10^{-3}		1.45×10^{-3}		1.26×10^{-3}		1.11×10^{-3}	
q_0	0.0894		0.0954		0.0993		0.0102	
b	25.8		0.773		1.21×10^{-2}		1.16×10^{-4}	
c	6.5	13	21	16	38	89	143	119
d	0.43	0.30	0.70	0.50	0.92	0.76	1.19	0.99
R_T/R_K	5.1	137	0.20	3.7	0.03	0.52	0.01	0.14
E_c/kT	36	55	24	33	19	24	16	19
C [fF]	0.26	0.17	0.39	0.28	0.49	0.39	0.59	0.49
f [MHz]	50	2.8	736	54.0	2990	244	7100	605
				Error level 10^{-9}				
R_TCf	1.13×10^{-3}		9.65×10^{-4}		8.38×10^{-4}		7.39×10^{-4}	
q_0	0.0730		0.0779		0.0811		0.0834	
b	38.7		1.16		1.82×10^{-2}		1.74×10^{-4}	
c	6.8	14	23	16	41	97	156	130
R_T/R_K	196	5310	2.26	42	0.21	3.2	0.04	0.62
E_c/kT	52	78	34	47	27	33	22	26
C [fF]	0.18	0.12	0.27	0.20	0.35	0.28	0.43	0.36
f [MHz]	1.25	0.069	61	4.7	450	36	1500	130

heating in the junctions[10] causes us not to expect device temperatures below 50–100 mK. We choose 100 mK as a conservative estimate. In Table III we have tabulated the parameters for two values of error $\mathcal{E} = 10^{-6}$, 10^{-9}, and the two values for the normalized voltage range $|u-q_0| = 0.1, 0.3$. We conclude from the table that for $N \geq 5$, devices with metrological accuracy are attainable with reasonable parameters.

Cotunneling errors can be easily suppressed by using large enough arrays of junctions. However, to reduce thermal errors, small state-of-the-art junctions ($\sim$0.2 fF) need to be made. The constraint on the maximum frequency will limit currents from the tens to possibly hundreds of picoamperes.

VII. SUMMARY

We calculate the accuracy of the pump analytically and with computer simulations for gate biasing that we think is optimal. Cotunneling arises from considering higher-order perturbation theory and is systematically calculated so that all possible cotunneling processes are included. Cotunneling rates are calculated using an approximation for the electron-hole excitation energies which evenly distributes the energies of the excitations. This is a better approximation than was previously made by disregarding the excitation energies altogether. Although the approximation is not valid at tunneling thresholds, the final accuracy formulas are not significantly affected.

We derive the thresholds for all tunneling processes. These results yield a simple graphical representation of cotunneling versus the bias parameters. The smallest errors occur in a bias region of $|U|C/e \lesssim 0.4$, where, at most, cotunneling of order $N-1$ occurs. We calculate analytical expressions for the rates of cotunneling. Both full and simple expressions of the errors are found.

We consider the effect of thermal activation of electrons over the Coulomb barrier, and derive expressions for the errors due to finite temperature. We consider the effect of operating the pump at too high a frequency and show that these errors occur from cotunneling processes of low order.

Our analytical predictions are in good agreement with computer calculations based on the master equation.

VIII. CONCLUSIONS

The accuracy of the pump can be calculated by considering the error sources of cotunneling, temperature, and frequency. The cotunneling errors can easily be made sufficiently small by making pump devices with five or more junctions. Small thermal errors require $E_c/k_BT \gtrsim 30$. The maximum operating frequency is approximately $5 \times 10^{-4}/(R_TC)$. This limits the maximum pump current from the tens to possibly hundreds of picoamperes.

We think pump devices with metrological accuracy can be built.

ACKNOWLEDGMENTS

We thank the members of the Quantronics Group of the CEA in Saclay, France, and especially D. Esteve for helpful discussions during the course of this work. This work was supported in part by the Office of Naval Research under Contract No. N00014-92-F-0003.

APPENDIX A: PROGRAM ALGORITHMS

A computer program has been written to calculate the current in the pump with nonzero gate capacitances and unequal values for the junction capacitance and resistances. The program uses the master equation and considers a subset of the system configuration when calculating the rates of all possible tunneling processes for each of these configurations. The dynamics of the system are determined by the master equation

$$\frac{dP}{dt} = \Gamma(U, \{U_g(t)\})P(t), \tag{A1}$$

where P is the probability vector, and Γ is the matrix of the transition rates which depend on the bias and gate voltages.

If we consider only piecewise constant functions for the gate voltages $U_g(t)$, the rate matrix is constant in each of these intervals, and we may readily solve the master equation for each such interval. We may write the solution as

$$P(t+\Delta t) = P(t)\exp(\Gamma \Delta t), \tag{A2}$$

where the exponential of the rate matrix is defined by the corresponding series expansion for a scalar argument. In the program we calculate the exponential of a matrix by using the eighth diagonal Padé table approximation[16] for the exponential function. This approximation gives an absolute error for $\exp(A)$ less than 10^{-10} for $||A|| < 1$. We use for Δt a value less than the inverse of the maximum rate occurring in the rate matrix. The calculation of the time evolution of the probability density vector P is then simply a series of vector-matrix multiplications and hence very fast.

The charge transferred through the device is calculated by keeping track of the rates of tunneling in each direction for each junction and for each state of the system, and then using

$$I_j(t) = e \sum_{\text{i=states}} \left(\gamma^i_{+j} - \gamma^i_{-j}\right) P_i(t), \tag{A3}$$

where $\gamma^i_{\pm j}$ are the accumulated rate out of state i through junction j in each of the directions. The charge transferred through each junction can be calculated by integrating Eq. (A3), using Eq. (A1), and the initial and final values of $P(t)$.

One may then check for self-consistency by comparing the currents flowing in each junction; vastly different currents correspond to charge flowing out of the state space from where it cannot return.

APPENDIX B: EXTENSION OF SINGLE-JUNCTION EVENTS

We may extend the picture of the stability region a bit further by considering the threshold lines for tunneling when junction $j+1$ is biased and the electron is on island $j-1$. This corresponds to the situation where the electron has not tunneled through junction j but junction j is being biased. This state is equivalent to a charge bias of Q around junction $j+1$ and a charge bias of e around junction j. We therefore need the expressions

$$Q_{xj} = e + \frac{-Q+UC}{N-1}, \tag{B1a}$$

$$Q_{x(j+1)} = Q + \frac{-e+UC}{N-1}, \tag{B1b}$$

$$Q_{xi} = \frac{-Q-e+UC}{N-1}, \quad i \neq j, j+1 \tag{B1c}$$

for the external charge of the three types of junctions. From these we can again derive the threshold lines for tunneling in each direction and for each of the three junction types.

APPENDIX C: RESETTING OF SWITCHING ERRORS

In the case of switching errors, we must also consider the processes through which the system relaxes to the new stable state. It is again straightforward to calculate the types and regions of the relaxations in the same manner as is calculated above for cotunneling.

As an example, assume junction j is biased and we have crossed the threshold for tunneling through junction j, but the electron has not yet tunneled. Let us assume the cotunneling process $\{+,+(n-1)\}$. The initial configuration is then described by the external charges of the junctions. Denoting the biased junction J, the unbiased junctions involved in the cotunneling process A, and the rest of the junctions B, we easily derive the external charges

$$Q_{xJ} = \frac{1}{N-1}[(N-1)(Q+e)+UC-(n-1)e], \tag{C1a}$$

$$Q_{xA} = \frac{1}{N-1}[-Q+UC+(N-1)e-(n-1)e], \tag{C1b}$$

$$Q_{xB} = \frac{1}{N-1}(-Q+UC-ne). \tag{C1c}$$

The system may now relax to the new stable state by two paths. In the first, the remaining junctions B may tunnel by cotunneling and/or by a cascade of single-junction events in the same direction as the initial cotunneling event; thus an extra electron is brought through the circuit. In the second, the unbiased junctions A may tunnel again but in the opposite direction thereby resetting the potential error. The biased junction will not tunnel again due to energy considerations.

In the first case, the ith single-junction tunneling event in k-order cotunneling in the forward direction will be given by

$$\delta E_i = \frac{e}{NC}\left(e\frac{N-1}{2} - Q + UC - ne - (i-1)e\right), \tag{C2}$$

and the total change in energy of such a continuation process is

$$\Delta E_k^{\text{cont}} = \sum_{i=1}^{k} \delta E_i = -\frac{e}{NC}k\left(Q - UC + ne - \frac{N-k}{2}e\right). \tag{C3}$$

This process is possible when $\Delta E_k < 0$ which occurs for

$$U\frac{C}{e} < \left[\frac{Q}{e} + n - \frac{N-k}{2}\right]. \tag{C4}$$

In the other case we similarly find for junctions belonging to set B and tunneling in the reverse direction

$$\Delta E_k^{\text{reset}} = \frac{e}{NC}k\left(Q - UC + ne - \frac{N+k}{2}e\right). \tag{C5}$$

There are two sets of threshold lines in the Q-U plane, one set for each direction. Within each set, the lines are separated by $\Delta U = e/2C$. One set is for tunneling in the same direction as the initial cotunneling process and shows where an extra electron is transferred through the circuit. The other set is for tunneling in the opposite direction and shows where the partial error process begun by the initial cotunnel process is reset. In general, the two processes are both possible and hence competing.

The other type of switching error does not relax in the same way. A switching error process involving only unbiased junctions tunneling in the reverse direction always relaxes by subsequently tunneling in the same direction. Switching errors involving the biased junction may relax in the two ways described above. Which type of process occurs depends, as is seen from Fig. 11, mainly on the bias voltage and the time dependence of Q.

*Permanent address: Danish Institute of Fundamental Metrology, DK-2800 Lyngby, Denmark.

[1]D. A. Averin and K. K. Likharev, in *SQUID '85*, edited by H.-D. Hahlbohm and H. Lübbig (de Gruyter, Berlin, 1985).
[2]D. A. Averin and K. K. Likharev, J. Low Temp. Phys. **62**, 345 (1986).
[3]K. K. Likharev, IBM J. Res. Develop. **32**, 144 (1988).
[4]T. A. Fulton and G. J. Dolan, Phys. Rev. Lett. **59**, 109 (1987).
[5]P. Delsing, K. K. Likharev, L. S. Kuzmin, and T. Claeson, Phys. Rev. Lett. **63**, 1861 (1991).
[6]L. J. Geerligs, V. F. Anderegg, P. A. M. Holweg, J. E. Mooij, H. Pothier, D. Esteve, C. Urbina, and M. H. Devoret, Phys. Rev. Lett. **64**, 2691 (1990).

[7]C. Urbina, H. Pothier, P. Lafarge, P. F. Orfila, D. Esteve, M. H. Devoret, L. J. Geerligs, V. F. Anderegg, P. A. M. Holweg, J. and E. Mooij, IEEE Trans. Magn. **27**, 2578 (1991); H. Pothier, P. Lafarge, C. Urbina, and M.H. Devoret, Europhys. Lett. **17**, 249 (1992).

[8]E. R. Willams, R. N. Ghosh, and J. M. Martinis, J. Res. Natl. Inst. Stand. Technol. **97**, 299 (1992).

[9]D. V. Averin and A. A. Odintsov, Phys. Lett. A **140**, 251 (1989).

[10]H. Pothier, Ph.D. thesis, University of Paris 6, 1991 (unpublished).

[11]Yu. V. Nazarov, Zh. Eksp. Teor. Fiz. **95**, 975 (1989) [Sov. Phys. JETP **68**, 561 (1989)]; M.H. Devoret, D. Esteve, H. Grabert, G.-L. Ingold, H. Pothier, and C. Urbina, Phys. Rev. Lett. **64**, 1824 (1990).

[12]G.-L. Ingold, P. Wyrowski, and H. Grabert, Z. Phys. B **85**, 443 (1991).

[13]K. K. Likharev, N. S. Bakhalov, G. S. Kazacha, and S. I. Serdyukova, IEEE Trans. Magn. **25**, 1436 (1989).

[14]D. V. Averin and Yu. V. Nazarov, Phys. Rev. Lett. **65**, 2446 (1990).

[15]V. Mel'nikov (private communication).

[16]G. H. Golub and C. F. Van Loan, *Matrix Computations*, (The John Hopkins University Press, London, 1989), pp. 555–560.

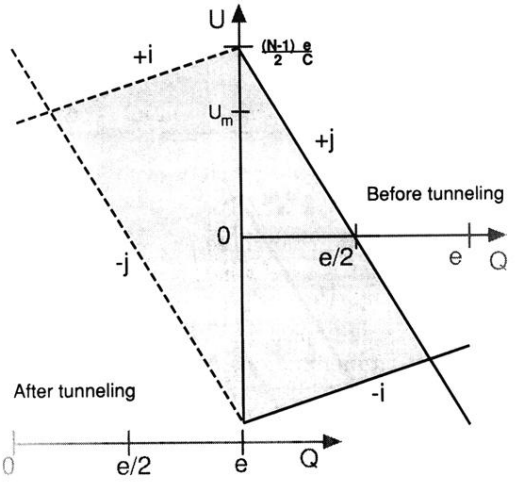

FIG. 10. Threshold lines for single-junction tunneling with gate bias Q and voltage bias U. The origin of the Q axis shifts by $-e$ when the biased junction tunnels; the threshold lines are correspondingly solid and dashed. The threshold lines for the biased junction are labeled $\pm j$, and for the unbiased junctions $\pm i$. The stability region for single-junction tunneling is shaded.

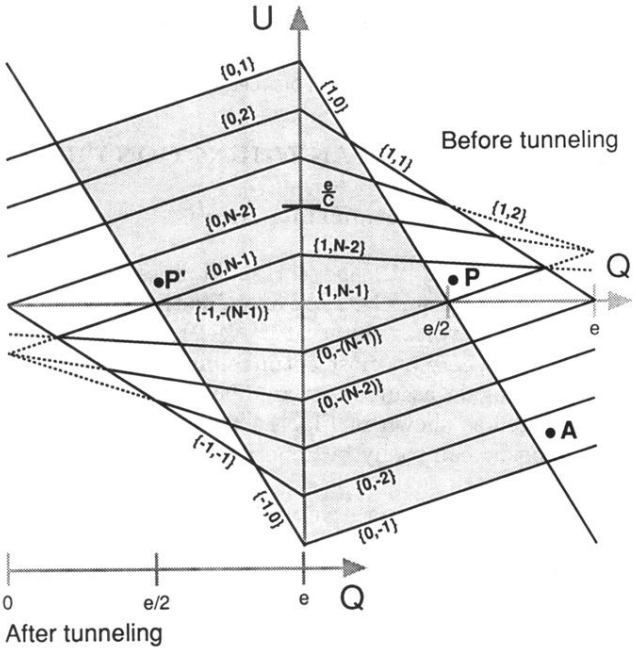

FIG. 11. Threshold lines for cotunneling, drawn similarly to Fig. 10. The lines are labeled with the type of process and are placed on the side of the threshold line where the process is allowed.

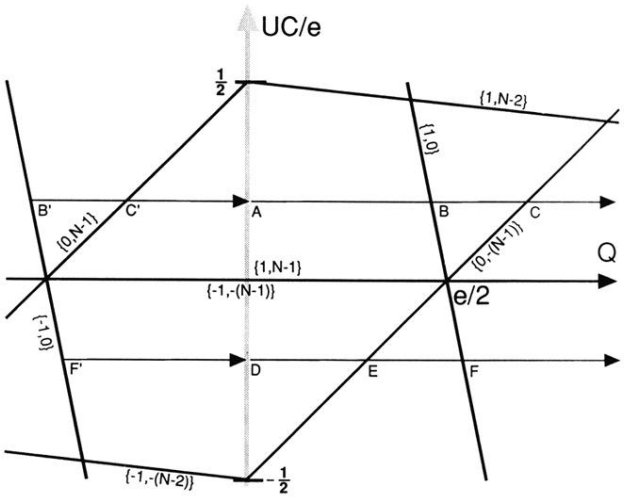

FIG. 12. The threshold lines of Fig. 11 around $U = 0$. Bias trajectories for the operation of the pump are lines parallel to the Q axis and are shown for positive and negative voltages.